

1 ***Quantifying the impact of lagged hydrological responses on the effectiveness of groundwater***  
2 ***conservation***

3  
4 **Authors:** Thomas J Glose<sup>1\*</sup>, Sam C Zipper<sup>1\*</sup>, David W Hyndman<sup>2,3</sup>, Anthony D Kendall<sup>3</sup>, Jillian  
5 M Deines<sup>4</sup>, James J Butler, Jr.<sup>1</sup>

6  
7 **Affiliations:**

8 1. Kansas Geological Survey, University of Kansas, Lawrence KS, 66047, USA

9 2. School of Natural Sciences and Mathematics, University of Texas at Dallas, Richardson, TX,  
10 75080, USA

11 3. Department of Earth and Environmental Sciences, Michigan State University, East Lansing,  
12 MI, 48824, USA

13 4. Energy and Environment Directorate, Pacific Northwest National Laboratory, Seattle, WA,  
14 98109, USA

15  
16 **\*Corresponding Author:** [tomglose@ku.edu](mailto:tomglose@ku.edu), [samzipper@ku.edu](mailto:samzipper@ku.edu)

17  
18 **Author ORCID IDs:**

19 Glose: 0000-0002-5414-3571

20 Zipper: 0000-0002-8735-5757

21 Hyndman: 0000-0001-9464-8403

22 Kendall: 0000-0003-3914-9964

23 Deines: 0000-0002-4279-8765

24 Butler: 0000-0002-6682-266X

25  
26 This is a manuscript in revision following peer review at *Water Resources Research*.

27  
28 **Keywords:** numerical modeling, lagged processes, groundwater conservation, pumping  
29 reductions, irrigation practices

30  
31 **Key Points:**

- 32 ● The long-term effectiveness of groundwater conservation initiatives based on pumping  
33 reductions is dependent on lagged processes
- 34 ● Vertical hydraulic conductivity ( $K_z$ ) controls if lagged responses are lateral-flow  
35 dominated or recharge-dominated
- 36 ● In our model, failure to account for lagged processes overestimates the median usable  
37 lifetime by 32 (lateral-flow-dominated) or 133 years (recharge-dominated)
- 38

39 **Abstract**

40 Many irrigated agricultural areas seek to prolong the lifetime of their groundwater  
41 resources by reducing pumping. However, it is unclear how lagged responses, such as reduced  
42 groundwater recharge caused by more efficient irrigation, may impact the long-term  
43 effectiveness of conservation initiatives. Here, we use a variably saturated, simplified surrogate  
44 groundwater model to: 1) analyze aquifer responses to pumping reductions, 2) quantify time lags  
45 between reductions and groundwater level responses, and 3) identify the physical controls on  
46 lagged responses. We explore a range of plausible model parameters for an area of the High  
47 Plains Aquifer (USA) where stakeholder-driven conservation has slowed groundwater depletion.  
48 We identify two types of lagged responses that reduce the long-term effectiveness of  
49 groundwater conservation, recharge-dominated and lateral-flow-dominated, with vertical  
50 hydraulic conductivity ( $K_z$ ) the major controlling variable. When high  $K_z$  allows percolation to  
51 reach the aquifer, more efficient irrigation reduces groundwater recharge. By contrast, when low  
52  $K_z$  impedes vertical flow, short term changes in recharge are negligible, but pumping reductions  
53 alter the lateral flow between the groundwater conservation area and the surrounding regions  
54 (lateral-flow-dominated response). For the modeled area, we found that a pumping reduction of  
55 30% resulted in median usable lifetime extensions of 20 or 25 years, depending on the dominant  
56 lagged response mechanism (recharge- vs. lateral-flow-dominated). These estimates are far  
57 shorter than estimates that do not account for lagged responses. Results indicate that  
58 conservation-based pumping reductions can extend aquifer lifetimes, but lagged responses can  
59 create a sizable difference between the initially perceived and actual long-term effectiveness.

## 60 **1. Introduction**

61           Irrigation uses the majority (69%) of fresh groundwater withdrawals in the United States  
62 (DeSimone et al., 2015; Dieter et al., 2018). In many aquifers supporting irrigated agriculture,  
63 heavy pumping has resulted in unsustainable water-level declines, threatening the economy and  
64 environment (Huggins et al., 2022; Deines et al., 2020; Scanlon et al., 2012). As groundwater is  
65 a limited resource, how to mitigate these declines to extend the usable lifetime of heavily  
66 stressed aquifers is a pressing question (Bierkens & Wada, 2019; Butler et al., 2020a; Castilla-  
67 Rho et al., 2019; Gleeson et al., 2020). In semi-arid environments with little access to surface  
68 water, groundwater conservation programs that seek to reduce pumping are one of the only  
69 viable options to decrease groundwater declines in the near to moderate term (Butler et al.,  
70 2020b; Deines et al., 2019; Hu et al., 2010).

71           The fundamental premise of groundwater conservation is to reduce outflows from the  
72 aquifer by reducing pumping. However, it is not clear how the effectiveness of such conservation  
73 initiatives might change in the future as the hydrological system in areas with groundwater  
74 conservation adjusts to the observed pumping reductions (Butler et al., 2020b; Deines et al.,  
75 2021; Foster et al., 2017). For example, the transit time for water at the land surface to percolate  
76 downward and become groundwater recharge can vary dramatically over the High Plains aquifer  
77 due to variations in unsaturated zone thickness and vertical hydraulic conductivity ( $K_z$ ), with  
78 estimates ranging from decades to centuries (Gurdak et al., 2008; Katz et al., 2016; McMahon et  
79 al., 2006; Zell & Sanford, 2020). Current management approaches are often implemented with a  
80 time horizon of years to decades (Miro & Famiglietti, 2019; Whittemore et al., 2018), while  
81 effective groundwater sustainability requires setting and meeting multi-generational goals  
82 (Gleeson et al., 2012). Evaluating groundwater conservation programs on multi-generational

83 timescales requires quantifying the long-term (decadal) response of aquifer water levels to  
84 pumping reductions.

85         The aquifer response to changes in pumping is a function of the pumping and a quantity  
86 termed net inflow, which is defined as total inflows (i.e., recharge, lateral inflows) minus all non-  
87 pumping outflows (i.e., discharge to streams, vegetation, lateral outflows), and is mediated by  
88 hydrostratigraphic characteristics such as hydraulic conductivity and specific yield (Butler et al.,  
89 2016). However, the relative contributions of vertical and lateral flows to net inflow are poorly  
90 understood and difficult to parse (Butler et al., 2016, 2020b). While recent work has found that  
91 reductions in aquifer net inflow can decrease the effectiveness of groundwater conservation  
92 programs over time (Butler et al., 2020b), the mechanisms, timescales, and variations in  
93 magnitudes of lagged responses from different water balance components is not known. As a  
94 result, we do not know which lagged responses may impact overall groundwater sustainability,  
95 nor the timescales and controlling processes.

96         To address this knowledge gap, we seek to answer the question: *How do lagged*  
97 *responses to pumping reductions impact the effectiveness of groundwater conservation practices*  
98 *over time?* We hypothesize that when groundwater conservation initiatives, such as Kansas'  
99 LEMA program, are enacted, (i) the reduction in pumping causes an immediate change to the  
100 aquifer water balance, leading to a slowing of the water table decline rate (Figure 1, light blue  
101 line); (ii) over time, inflows will diminish because more efficient irrigation will lead to a  
102 reduction in deep percolation (water that drains below the rooting zone; Deines et al., 2021),  
103 which will eventually reduce recharge to the aquifer. Similarly, lateral inflow to the conservation  
104 area will diminish, as decreased pumping will reduce the hydraulic gradient driving water into  
105 the area. In both situations, the result will be an increase in water table decline rates to an

106 intermediate rate between the pre-conservation decline rate and the immediate post-conservation  
107 rate (dark blue line in Figure 1).

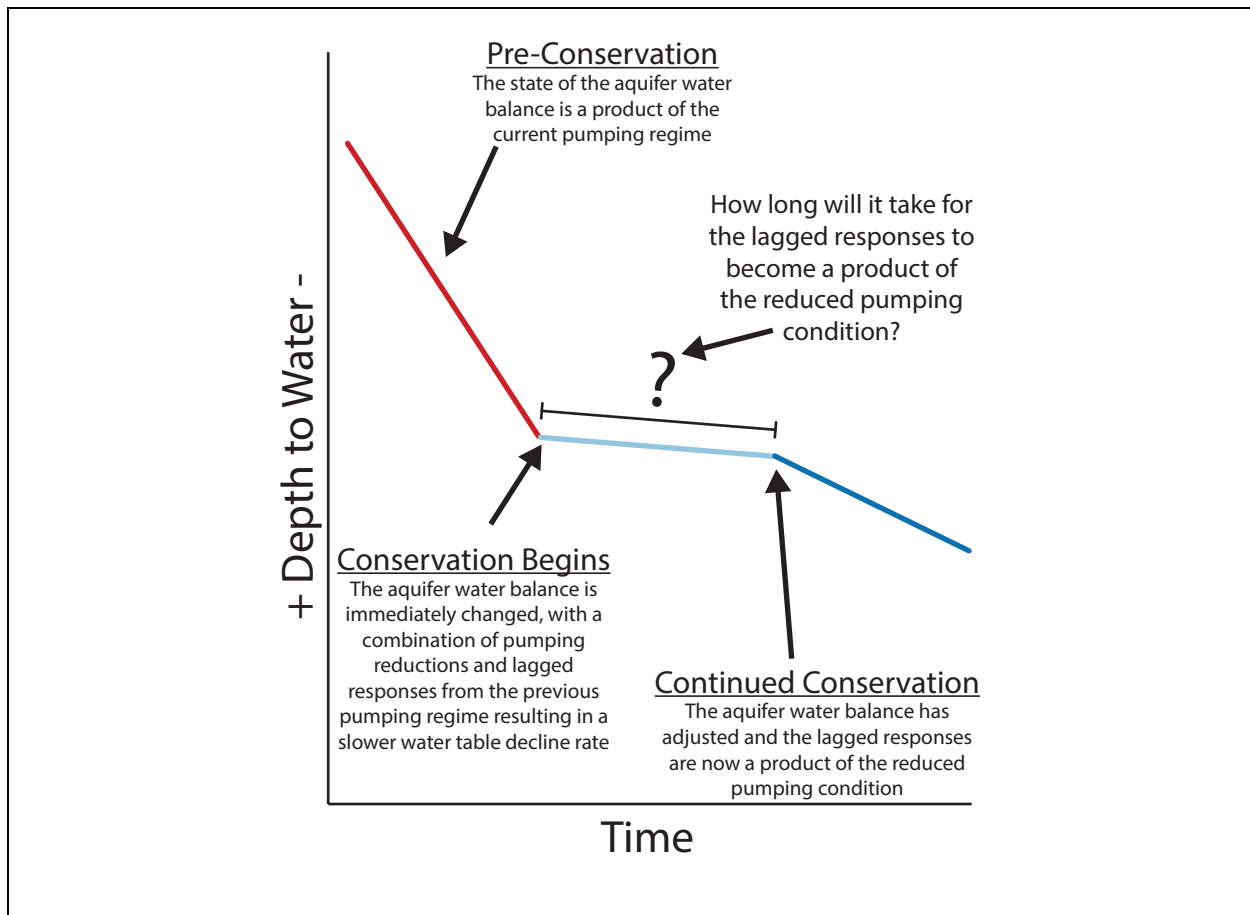


Figure 1: Graphical representation of hypothesized aquifer water balance changes due to pumping reductions. The initial reduction in pumping causes an immediate change to the aquifer water balance, resulting in an initial period of high effectiveness (light blue line) that wanes in time as lagged responses, such as groundwater recharge and lateral flow, adjust to the new pumping regime (dark blue line).

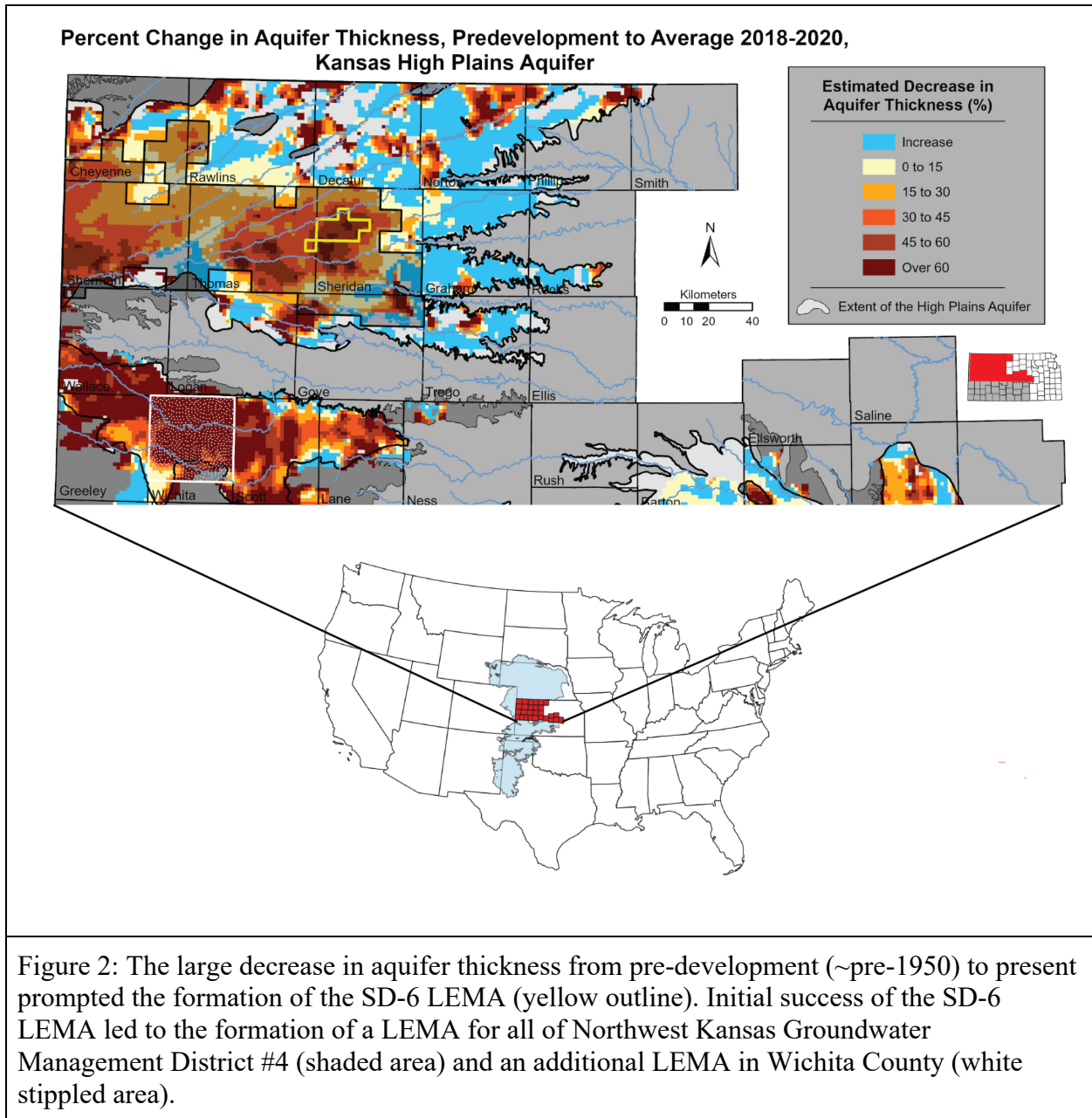
108 To test these hypotheses, we developed a variably saturated groundwater flow model for  
109 the SD-6 LEMA based on historical observations and realistic conditions. To ensure that results  
110 were not reflective of site-specific phenomena, we employed a simplified surrogate modeling  
111 approach. We used this model to evaluate the long-term changes in the aquifer water balance  
112 associated with groundwater conservation, quantify the implications of lagged responses for

113 estimates of usable aquifer lifetimes, and determine the physical controls on these lagged  
114 responses.

## 115 **2. Methods**

### 116 ***2.1 Study region***

117 We used the Sheridan-6 Local Enhanced Management Area (SD-6 LEMA) in Kansas as  
118 a representative groundwater conservation program to evaluate these hypotheses. Located within  
119 the portion of the High Plains aquifer in northwestern Kansas, the SD-6 LEMA overlies a thick  
120 section of highly transmissive, unconsolidated sediments. There are no sources of surface water  
121 in the region and therefore groundwater is heavily pumped to support irrigated agriculture  
122 (Whittemore et al., 2018). LEMAs are a stakeholder-driven governance approach in which  
123 groundwater users (primarily irrigators) and groundwater management districts develop  
124 conservation plans. Once approved by the state, LEMAs are enforced by the state regulatory  
125 agency (Kansas Statutes Annotated 82a-1041, 2012). SD-6, the state's first LEMA, was initiated  
126 in 2013 in a 255-km<sup>2</sup> area in northwest Kansas with the stated goal of reducing annual pumping  
127 by 20% over a five-year period (Figure 2, yellow outline). During that period, irrigators  
128 exceeded their goal, reducing pumping by 31% on average and slowing water table decline rates  
129 while maintaining similar economic returns (Deines et al., 2019, 2021; Golden, 2018;  
130 Whittemore et al., 2018). This initial success led to an extension of the SD-6 LEMA for an  
131 additional five years, the 2018 formation of a much larger LEMA that encompasses most of the  
132 northwest Kansas portion of the High Plains aquifer (Northwest Kansas Groundwater  
133 Management District #4) (Figure 2, shaded area), and an additional 2021-initiated LEMA in  
134 west-central Kansas (Kansas Department of Agriculture, 2013, 2018, 2021) (Figure 2, white  
135 stippled area).

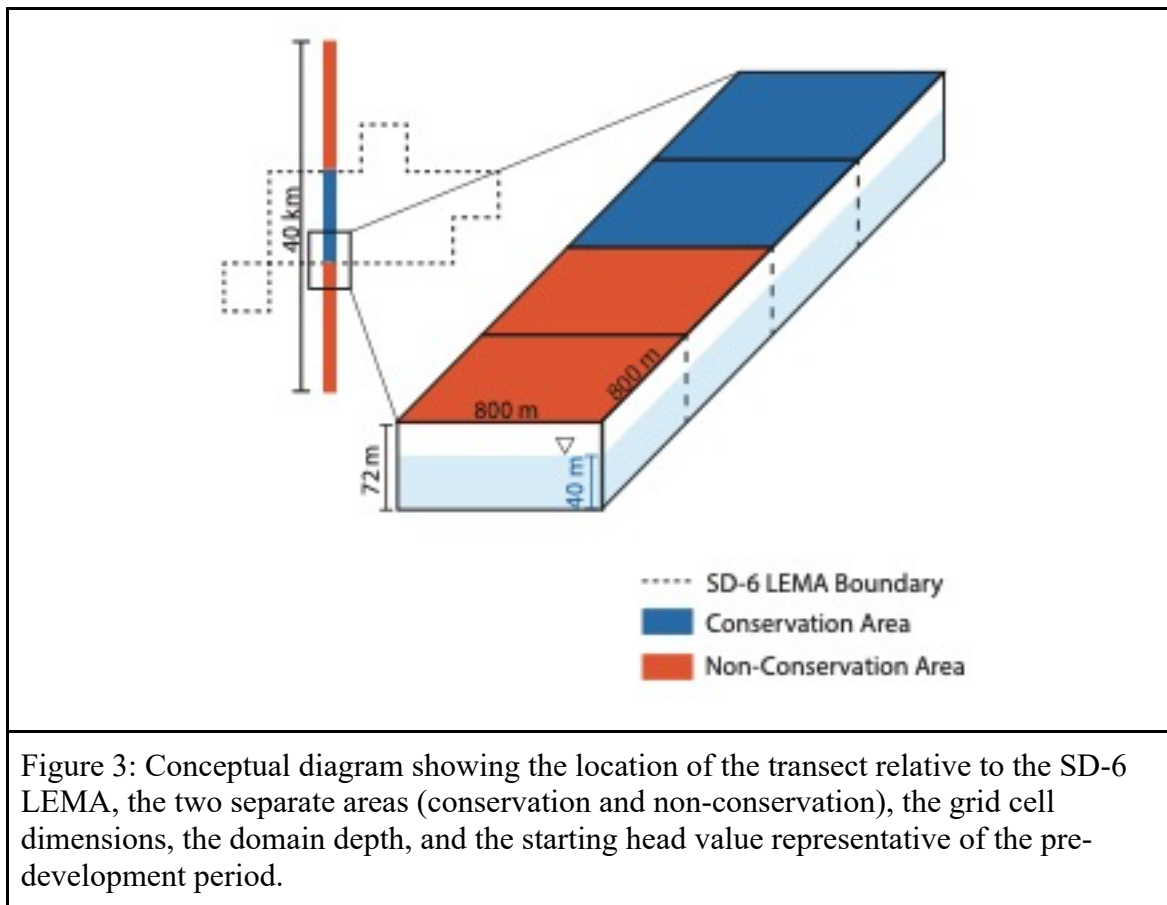


136

137 **2.2 Model Overview**

138 To test our hypotheses, we developed a variably saturated groundwater flow model of an  
 139 arbitrary north-south linear transect that passes through the SD-6 LEMA (Figure 3). We elected  
 140 to build a simplified model, rather than a fully-calibrated three-dimensional groundwater flow  
 141 model, to better isolate the hydrological processes of interest, and more directly test our

142 hypotheses by avoiding unnecessary site-specific complexity--an approach known as surrogate  
143 or archetypal modeling (Asher et al., 2015; Razavi et al., 2012; Voss, 2011a, 2011b; Zipper et  
144 al., 2018, 2019). Nevertheless, to ensure our model provided a reasonable simulation of the  
145 dominant processes in this region, we conducted an evaluation against field data from the SD-6  
146 region, and conducted a sensitivity analysis to test the impact of simplifying assumptions on  
147 model results.



148

### 149 **2.3 Model Construction and Input Data**

150 We used the United States Geological Survey's MODFLOW-NWT program and  
151 constructed the model using the Python package FloPy (Bakker et al., 2016). The 40 km long  
152 domain consists of a single layer of 50 grid cells, each 800 m by 800 m in size, covering a total

153 area of 32 km<sup>2</sup>. Each grid cell is roughly equivalent in area to a typical field size in the region  
154 (64.75 hectares [160 acres]) and cell dimensions were set based on the typical distance between  
155 irrigation wells in the area to match spatial patterns of water withdrawals in the area (Figure S1).  
156 The model domain was split into two types of management practices (conservation and non-  
157 conservation; blue and orange areas, respectively, in Figure 3), which were represented in the  
158 model using different pumping and deep percolation rates as described below. The conservation  
159 area was made up of 14 grid cells while the non-conservation areas each consisted of 18 grid  
160 cells, with the four additional cells being added to remove the influence of edge effects from the  
161 northern and southern no-flow boundaries. The single model layer is 72 m thick and starting  
162 pressure heads were set to 40 m; these values represent the average depth to bedrock and  
163 pressure heads, respectively, of the area for the pre-development period (~pre-1950) (Fross et al.,  
164 2012). The top of the model is assumed to be below the rooting zone to remove the influence of  
165 evapotranspiration, overland flow, and discharge to surface water bodies. Regional groundwater  
166 flow is perpendicular to our transect from west to east (Fross et al., 2012, Figure S2), so we  
167 included a lateral flow boundary condition on the west side and a no-flow boundary on the east  
168 to represent the net lateral flow entering the modeled area, which is distinct from the vertical  
169 inflow from groundwater recharge. Since our model is a north-south transect, this approach  
170 reduces the number of uncertain parameters by lumping inflow from the west and outflow to the  
171 east into a single net lateral inflow term. We varied net lateral flows along with the model  
172 hydrostratigraphic properties as described in Section 2.4.

173           Pumping and deep percolation rate time series were developed using a combination of  
174 historical annual precipitation depth, regression model-based historical pumping data (1955-  
175 1992) (Wilson et al., 2005), and measured pumping volumes (1993-2018). We estimated annual

176 pumping volumes by establishing relationships between annual areally averaged precipitation  
 177 depth and applied irrigation depth during the 2000-2018 period, the period after a large majority  
 178 of irrigators had transitioned from traditional high pressure center pivot irrigation to more  
 179 efficient center pivot with drop nozzle irrigation (Figure 4a) (Pfeiffer & Lin, 2010; Rogers &  
 180 Lamm, 2012).

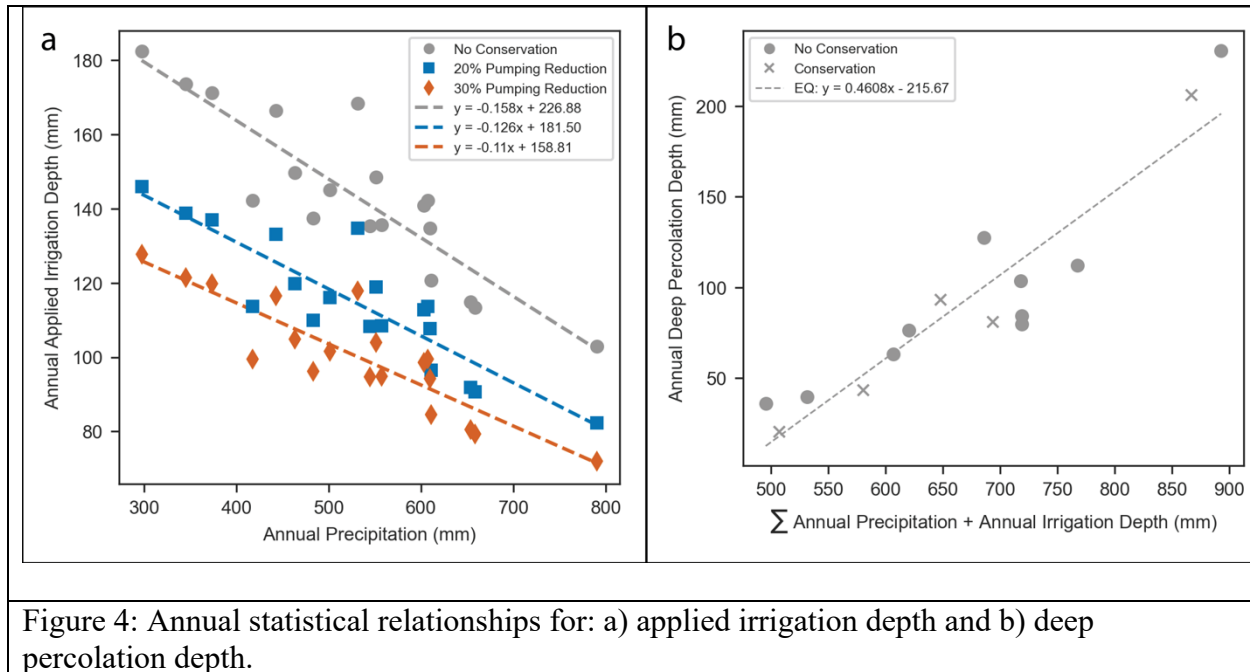


Figure 4: Annual statistical relationships for: a) applied irrigation depth and b) deep percolation depth.

181  
 182 We first estimated annual areally averaged applied irrigation depth as the total pumping volume  
 183 from wells within SD-6 divided by the total area. Observed pumping rates from the SD-6 LEMA  
 184 were modified to account for the climate-adjusted 27% reduction in pumped volume observed  
 185 during the first four years of the LEMA using the approach of Whittemore et al. (2018) and  
 186 Butler et al. (2020b). We then developed a relationship between precipitation and irrigation  
 187 depth for the “No Conservation” portions of the domain that included the period after the  
 188 establishment of the SD-6 LEMA (2000-2018). We developed two additional relationships to  
 189 simulate conservation practices by modifying the “No Conservation” relationship (Figure 4a): (i)

190 a 20% pumping reduction scenario based on the legal requirements for the SD-6 LEMA; and (ii)  
191 a 30% pumping reduction scenario that more closely reflects observed irrigator behavior.

192 For each pumping scenario, we then calculated the applied pumping volume for each grid  
193 cell as the product of irrigation depth from the statistical relationship (Figure 4a) and the area of  
194 the grid cell. We disaggregated the estimated annual pumping volume uniformly over a 103-day  
195 period, which was the average time between the onset and cessation of irrigation pumping in the  
196 region interpreted from high temporal-resolution well observations (Butler et al., 2019). Pumping  
197 was simulated using MODFLOW's well (WEL) package. As discussed in Section 2.2, our  
198 surrogate modeling approach was not intended to precisely represent observed spatial pumping  
199 dynamics within the SD-6 LEMA, but rather the average aquifer response to typical regional  
200 pumping. To reflect that the estimated pumping volume is representative of the entire SD-6 area,  
201 which is heavily irrigated, we placed a pumping well in each individual grid cell both inside and  
202 outside the conservation area. Due to the small amount of north-south variation in precipitation  
203 in our study domain (Figure S3), we used the same precipitation for estimating pumping in all  
204 grid cells so pumping was initially uniform within the conservation and non-conservation areas.

205 The model simulated flow through variably saturated porous media using the unsaturated  
206 zone flow (UZF) package, which uses a kinematic-wave approximation to solve the 1-D  
207 Richard's equation (Niswonger et al., 2006; Smith, 1983; Smith & Hebbert, 1983). While  
208 numerous models can simulate variably saturated flow, the UZF package for MODFLOW has  
209 several advantages for our purposes, including documented applications in thick vadose zones  
210 (Hunt et al., 2008; Nazarieh et al., 2018), computational efficiency (Kennedy et al., 2016;  
211 Niswonger & Prudic, 2009), and widespread use (Bailey et al., 2013; Hou et al., 2020; Morway  
212 et al., 2013). Since the top of our model domain represents the bottom of the root zone, we

213 provided UZF with annual values of deep percolation from a linear model fit between simulated  
214 deep percolation from a calibrated crop model for the SD-6 area with and without conservation  
215 (Deines et al., 2021), and the sum of annual precipitation and applied irrigation depth following  
216 Scanlon et al. (2006) (Figure 4b). Like pumping, annual deep percolation values were uniformly  
217 disaggregated to daily values over the 103-day pumping period, since water inputs to the soil  
218 column (both precipitation and irrigation) are primarily concentrated during the growing season.  
219 The SALUS model that generated the deep percolation estimates simulates the root zone water  
220 balance including precipitation, evaporation, root water uptake, and irrigation, with irrigation  
221 being the dominant driver of deep percolation rates during the pumping season (Deines et al.,  
222 2021). Unlike the separate relationships required for pumping under each conservation scenario,  
223 only one relationship is needed to estimate deep percolation because the effects of groundwater  
224 conservation are accounted for in the annual irrigation depth term. These relationships (Figures  
225 4a and 4b) were used to generate deep percolation rate time series for both the evaluation and  
226 projection periods as well as pumping rate time series for the projection period (Figure 5).  
227 Pumping rate time series for the evaluation period were generated using a combination of  
228 regression model-based and measured pumping rates.

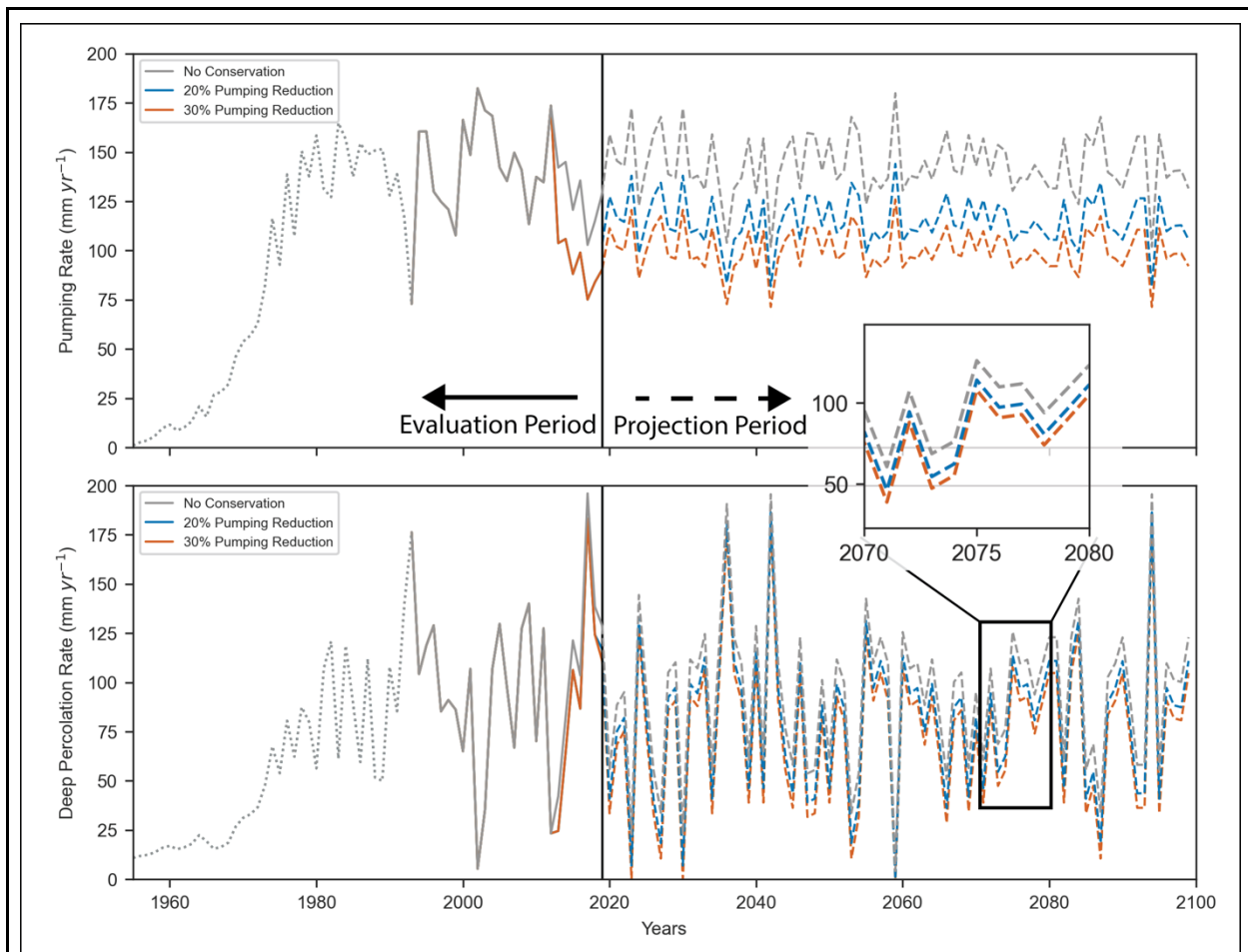


Figure 5: Pumping (upper) and deep percolation (lower) rates calculated from the statistical relationships in Figure 4. For the three very dry years in the prediction period, the statistical relationship in Figure 4b produced negative deep percolation rates; these years were assigned a rate of 0 m d<sup>-1</sup>. For the historical period, pumping rate and deep percolation are shown only for the 30% pumping reduction scenario (orange) as this best represents observed irrigator behavior.

229 Our simulations spanned 201 years (1900-2100), which can be divided into three periods:  
 230 spin-up (1900-1954), historical (1955-2019), and projection (2020-2100). The 55-year spin-up  
 231 period is prior to the onset of high capacity pumping in the region so the only fluxes in/out of the  
 232 domain are deep percolation, which was applied at a rate of  $5 \times 10^{-4}$  m d<sup>-1</sup> (51.5 mm yr<sup>-1</sup>) to  
 233 approximate pre-development recharge in the area (Fross et al., 2012; Hansen, 1991), and the  
 234 applied lateral inflows. To ensure that recharge and lateral inflow did not change the prescribed  
 235 pre-development saturated zone pressure heads, a drain was placed at the pre-development water

236 level (40 m) across the domain. This approximates the effect of the regional streams that drained  
237 the system during the pre-development period. After the spin up period, a mix of regression-  
238 estimated (1955 to 1992) (Wilson et al., 2005) and measured pumping volumes (1993 to 2018)  
239 for the SD-6 area was used to define pumping rate inputs for the model (Figure 5). Pumping data  
240 for the year 2019 was estimated using the statistical regression as pumping data were not  
241 available, but this year was included in the evaluation period as water level change and head data  
242 were available at the time of model development. As observed irrigator behavior within the  
243 LEMA was close to the 30% pumping reduction scenario, we used the 30% reduction pumping  
244 rates for 2013-2019. The projection period (2020-2100) allows us to evaluate the long-term  
245 implications of pumping with the baseline and the two reduction (20% and 30%) pumping  
246 scenarios. For the projection period, we randomly sampled annual precipitation from the  
247 historical precipitation record to estimate pumping and deep percolation for each year based on  
248 the relationships shown in Figure 4 since there are no consistent long-term historical (Lin et al.,  
249 2017) or projected (Figure S4) precipitation trends in this region, and historical precipitation  
250 patterns do not exhibit significant temporal autocorrelation (Butler et al., 2020b).

#### 251 ***2.4 Model Evaluation and Evaluation of Control Parameters***

252 We used a Latin hypercube sampling scheme (McKay et al., 1979) to identify the model  
253 parameters that best reproduced observed hydrological data, and evaluate the sensitivity of  
254 model output to each parameter and the interactions between parameters (Zipper et al., 2018).  
255 Our Latin hypercube sample consisted of 2,000 near-random, unique sets of hydrostratigraphic  
256 parameters (vertical saturated hydraulic conductivity,  $K_z$ ; specific yield,  $S_Y$ ; Brooks and Corey  
257 epsilon,  $\epsilon$ ) and lateral inflow (LI), which were selected from a uniform distribution over the  
258 parameter space shown in Table 1. We ran one simulation using each parameter set to explore

259 lagged responses to groundwater conservation across a range of hydrogeological settings and to  
 260 reduce the risk of identifying a local optimum as the best parameter set.

Table 1: Parameter space ranges for the Latin hypercube sampling scheme. As we are taking a surrogate modeling approach, ranges were extended outside of their observed values for the area to allow the parameter space to be fully explored. <sup>1</sup>(Fross et al., 2012) <sup>2</sup>(Butler et al., 2016), <sup>3</sup>(Brooks & Corey, 1966)

<b>Parameter</b>	<b>Lower Bound</b>	<b>Upper Bound</b>
<b>log<sub>10</sub> Vertical Hydraulic Conductivity (m d<sup>-1</sup>)<sup>[1]</sup></b>	-6	1
<b>Specific Yield (-)<sup>[2]</sup></b>	0.06	0.18
<b>Brooks and Corey Epsilon (-)<sup>[3]</sup></b>	2	5
<b>log<sub>10</sub> Lateral Inflows (m d<sup>-1</sup>)<sup>[2]</sup></b>	-6	-3

261  
 262 Horizontal hydraulic conductivity and saturated water content were held constant at 20 m  
 263 d<sup>-1</sup> and 0.25, respectively, to reflect average values in the SD-6 LEMA area (Fross et al., 2012).  
 264 The UZF package relies on the Brooks and Corey function to calculate unsaturated K<sub>Z</sub> (Brooks  
 265 & Corey, 1966). This function requires residual water content, here approximated for each  
 266 parameter set by taking the S<sub>Y</sub> value for each set and subtracting it from the saturated water  
 267 content (Niswonger et al., 2006). A value of 0.005 was added to the calculated residual water  
 268 content to ensure that the unsaturated hydraulic conductivity value did not start at a value of  
 269 zero.

270 We evaluated the performance of each of the 2000 simulations via comparison to the  
 271 observed groundwater level data for the 1999-2019 period, which represents the longest  
 272 continuous record of reliable observations within the SD-6 LEMA (KGS WIZARD Database;

273 <http://www.kgs.ku.edu/Magellan/WaterLevels/index.html>). The goal of this study is to ensure  
274 that the dominant processes (e.g., pumping reductions and lagged responses) are appropriately  
275 simulated while not overparameterizing the model since our focus is not on site-specific  
276 heterogeneity (Konikow & Bredehoeft, 1992).

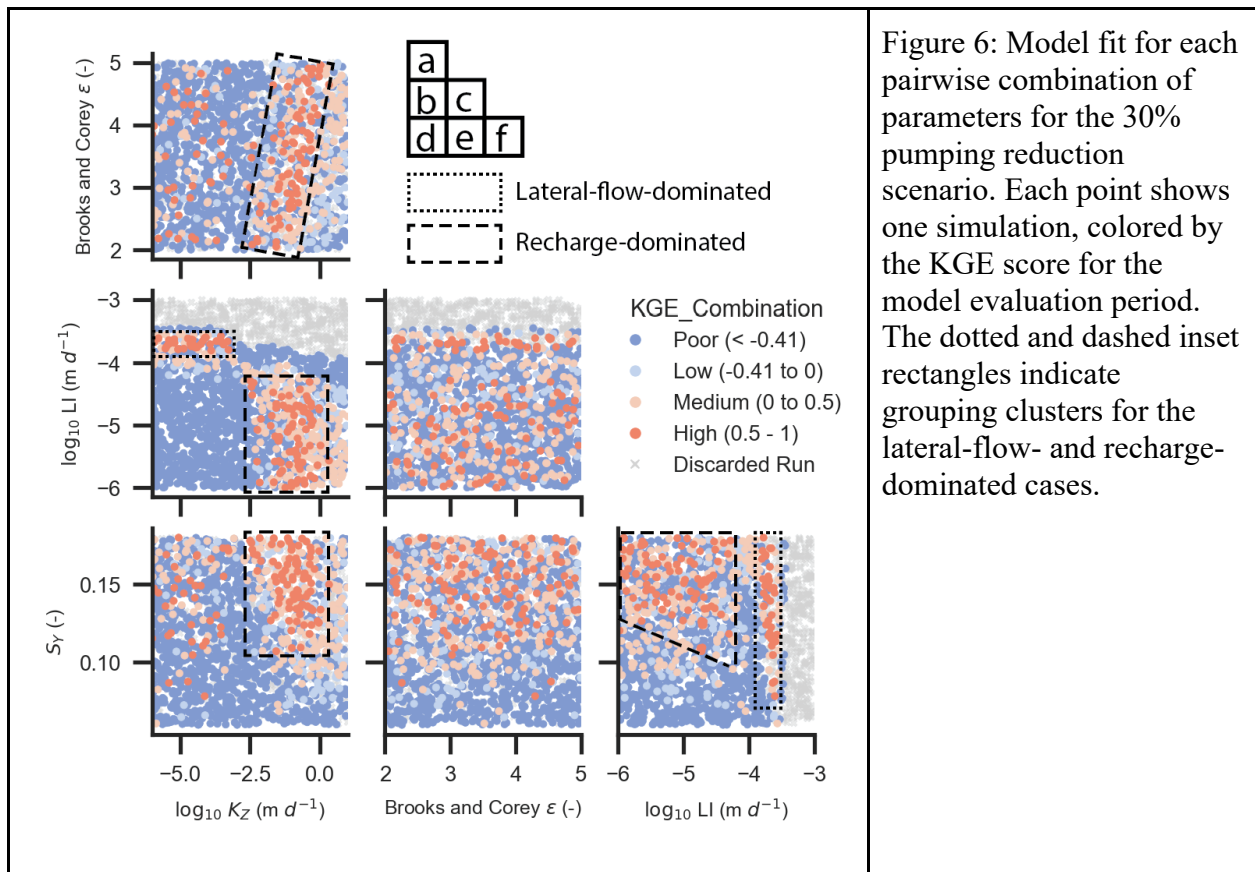
277         We quantified model performance for each parameter set using a two-step approach.  
278 First, as the area has experienced significant drawdown, we eliminated model runs in which the  
279 head in the model domain at the end of the historical period (2019) was still at or above pre-  
280 development levels (Fross et al., 2012). For the remaining runs, we calculated the Kling-Gupta  
281 Efficiency (KGE; Kling et al., 2012) score for both the annual water table elevation and the  
282 interannual change in water table elevation, which are based on measurements taken each  
283 January in the LEMA area. We selected these two metrics to ensure that both the long-term and  
284 interannual dynamics were simulated reasonably, and used the minimum (lower-performing) of  
285 these two KGE values as the final KGE score for that parameter set. We then divided the model  
286 runs into four performance groups: poor ( $KGE < -0.41$ , which indicates that the model results are  
287 worse than the mean of the observations; Knoben et al., 2019), low ( $-0.41 < KGE < 0$ ), medium  
288 ( $0 < KGE < 0.5$ ), and high ( $KGE > 0.5$ ). A KGE score of 1 would indicate a perfect match  
289 between a simulation and observations. Only runs in the high performance group were analyzed  
290 for the projection period because those parameter sets were able to reasonably approximate  
291 historical hydrological conditions. We also conducted a sensitivity analysis to determine the  
292 influence of several simplifying assumptions (model discretization, model homogeneity, uniform  
293 distribution of pumping wells) on model results. To do this, we ran five additional model  
294 scenarios with a smaller grid cell dimension in which each simplification was analyzed further  
295 (see Text S1, Figure S5, and Table S1 for more details).

296 The models selected for projection were run to the year 2100 and the extension of the  
 297 usable aquifer lifetime was quantified for the 20% and 30% pumping reduction scenarios. For  
 298 each parameter combination and pumping scenario, the extension of the usable aquifer lifetime is  
 299 calculated as the number of years that water levels in the aquifer remain above a minimum  
 300 threshold relative to the baseline “No Conservation” scenario. For this region, we assumed that a  
 301 minimum saturated thickness of eight meters is required for large-scale irrigation to allow for  
 302 sufficient transmissivity, and therefore well yield, along with pumping-induced drawdown in the  
 303 well (Deines et al., 2020; Butler et al., 2020b).

304

### 305 3. Results and Discussion

#### 306 3.1 Recharge and lateral flow-dominated inflows



307 We found that many parameter combinations were able to reproduce the historical head  
308 and head change observations (Figure 6). Of the 2,000 parameter combinations tested, there were  
309 122 simulations rated as high performance (Figure 6, dark red circles, KGE > 0.5). An additional  
310 214 were rated as medium, 126 as low, 1,090 as poor, and 448 were discarded due to no  
311 simulated drawdown (Figure 6). Within parameter pairs, there are several clusters that occur  
312 throughout the parameter space (Figure 6b), the most evident occurring between lateral inflow  
313 (LI) and vertical hydraulic conductivity ( $K_Z$ ). In parameter space, these two clusters correspond  
314 to a high LI/low  $K_Z$  zone, in which lateral groundwater flow is the dominant inflow to the  
315 aquifer, and a low LI/high  $K_Z$  zone, in which vertical groundwater recharge is the dominant  
316 inflow to the aquifer. Since each plot represents the combination of two variables, subplots with  
317 intermingled high and low performing model runs (i.e., Figure 6c and 6e) indicate that those  
318 variables have a relatively low influence on simulated groundwater response to pumping and  
319 conservation and that model performance is primarily controlled by other variables. In contrast,  
320 variable combinations that have a strong influence on simulated results (i.e., Figure 6b) show a  
321 clearer separation of high and low performing model runs.

322 For the lateral-flow-dominated case, the parameter sets that yield high KGE scores have  
323 LI values between  $1.6 \times 10^{-4}$  and  $2.5 \times 10^{-4}$  m d<sup>-1</sup> and  $K_Z$  values between  $1 \times 10^{-6}$  (the lower  
324 bound of the parameter space tested) and  $5 \times 10^{-4}$  m d<sup>-1</sup>. However, for the Brooks and Corey  $\epsilon$   
325 and  $S_Y$  there are no clear thresholds, indicating that the rate of lateral flow is the controlling  
326 factor. The ranges of  $K_Z$  and LI values with good fits in the recharge-dominated case are  
327 opposite of the lateral-flow-dominated case, with higher  $K_Z$  values (from  $3.5 \times 10^{-3}$  to 1 m d<sup>-1</sup>)  
328 and lower LI values (from  $5 \times 10^{-5}$  m d<sup>-1</sup> to the lower bound of the parameter space tested,  $1 \times 10^{-6}$   
329 m d<sup>-1</sup>) (Figure 6b). In contrast to the lateral-flow-dominated case, the recharge-dominated case

330 is also sensitive to the Brooks and Corey  $\epsilon$  and  $S_Y$ . As  $K_Z$  approaches  $1 \text{ m d}^{-1}$ , the value of  $\epsilon$   
 331 steadily increases from 2 to 5 (Figure 6a). The range of  $S_Y$  is also limited based on  $K_Z$ , with  $S_Y$   
 332 values between 0.1 and 0.18 necessary to generate KGE scores of  $\geq 0.5$  (Figure 6d). Vertical  
 333 hydraulic conductivity is not the only controlling factor in the recharge-dominated case. As the  
 334 value of LI increases towards its upper limit of  $5 \times 10^{-5} \text{ m d}^{-1}$ , the range of  $S_Y$  also expands with  
 335 its lower limit dropping from 0.13 to 0.1 (Figure 6f). The interplay between hydrostratigraphic  
 336 parameters plays a more prominent role in the recharge-dominated scenario. Along with  $K_Z$ , the  
 337 Brooks and Corey  $\epsilon$  and  $S_Y$  influence the rate and volume of vertical water movement through  
 338 the thick vadose zone, respectively, and therefore influence the performance of the model.

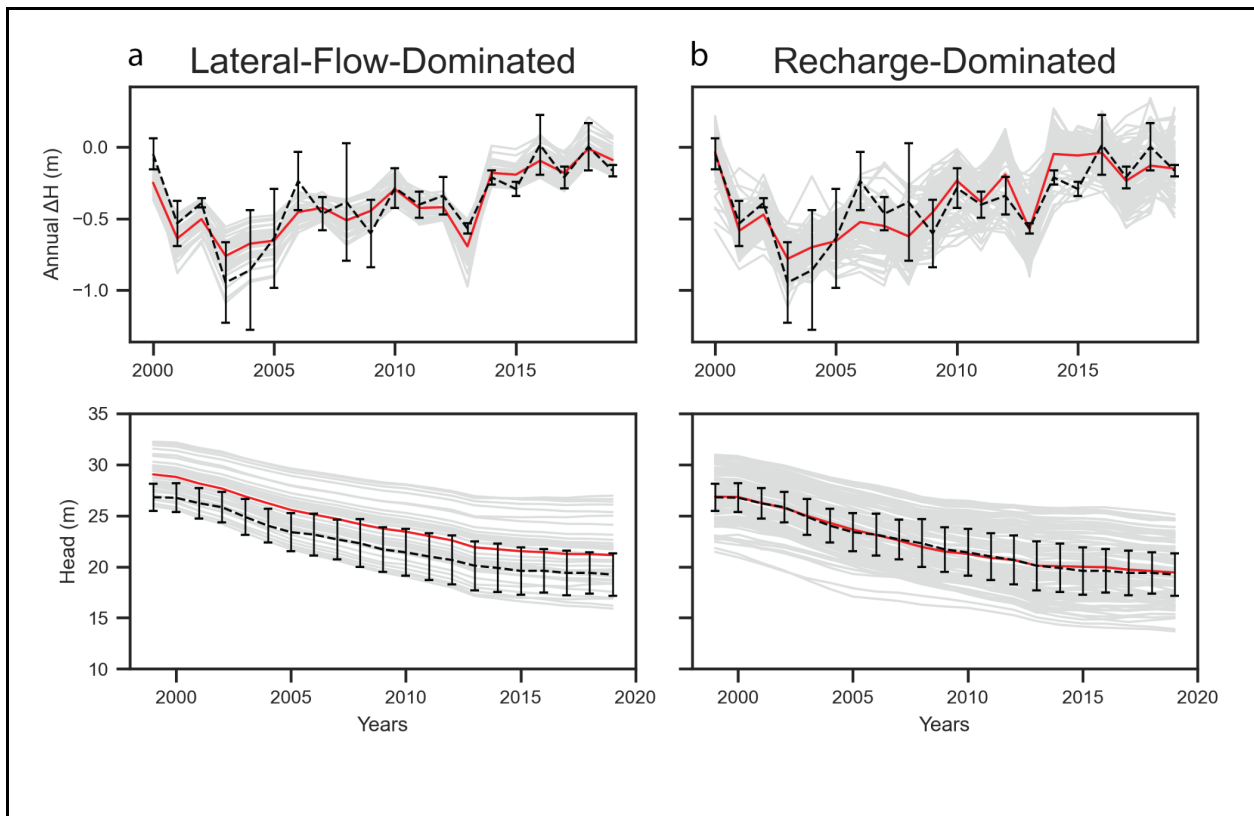


Figure 7: Results for the 30% pumping reduction scenario of observed (black, dashed line), simulated (light gray, solid lines), and average simulated (red lines) interannual change in pressure head and annual pressure head values for the a) lateral-flow-dominated and b) recharge-dominated cases. Simulation results presented for the center cell in the conservation area, the error bars show one standard deviation about the mean of the observed data.

340 For both the lateral-flow-dominated and recharge-dominated cases, the average simulated  
341 interannual change in pressure head and annual pressure head values (Figure 7a, b, red lines)  
342 reasonably align to the average observed values (Figure 7a, b, dashed lines), indicating that the  
343 model is reasonably capturing the annual and interannual dynamics of the natural system. While  
344 the recharge-dominated simulations are closer to the mean of the observed head values, lateral-  
345 flow-dominated simulations were generally within one standard deviation of the mean of all  
346 observations and better matched observed interannual head change. The average KGE score and  
347 root mean square error (RMSE) were quantified for all high-performing lateral-flow- and  
348 recharge-dominated runs. In the lateral-flow-dominated cases the KGE score and RMSE for the  
349 interannual change in head are 0.687 and 0.142 m, respectively. For the annual head, these  
350 values are 0.776 and 2.226 m, respectively. In the recharge-dominated cases the KGE score and  
351 RMSE for the interannual change in head are 0.644 and 0.205 m, respectively. For the annual  
352 head, these values are 0.763 and 2.507 m, respectively. We also tested the sensitivity of our  
353 model results to several of the simplifying assumptions adopted in our surrogate modeling  
354 approach: model discretization, model homogeneity, uniform distribution of pumping wells. We  
355 found that increasing the complexity of our model did not substantially affect our results or  
356 interpretations (Text S1, Figure S5, Table S1).

357 The wide variety of parameters that lead to reasonable agreement with the observed data  
358 indicates that multiple interpretations of the underlying processes that dictate groundwater  
359 recharge in areas with thick vadose zones are equally valid, following the principle of  
360 equifinality (Beven, 2006). In groundwater modeling, parameter estimation often seeks to find a  
361 local or global optimum to match limited observations while minimizing an objective function  
362 using software such as PEST (Doherty, 2015) or UCODE (Poeter & Hill, 1999). However, the

363 hunt for an ideal parameter set that results in simulated values closely matching observed values  
364 can ignore other possible parameter sets that perform nearly equally well (Savenije, 2001; Liu et  
365 al., 2022). This is true for our surrogate model of the SD-6 area as the lack of vadose zone  
366 observation data paired with an exploration of a wide parameter space resulted in two possible  
367 and equally valid mechanisms, or combination of mechanisms, that affect the long term  
368 performance of pumping reduction-based groundwater conservation initiatives. In practice, these  
369 two end members define a spectrum and the actual setting is found somewhere on this spectrum.  
370 Since the long-term response of an aquifer to pumping and conservation will be dictated by the  
371 relative magnitude of each of these processes, this further highlights the need to better  
372 understand when each of these lagged processes is dominant.

### 373 *3.2 Lagged responses to conservation in recharge- and lateral flow-dominated conditions*

374 Recharge-dominated and lateral-flow-dominated cases exhibit different long-term  
375 hydrological responses to groundwater conservation due to differences in lagged changes to the  
376 aquifer water balance. In lateral-flow-dominated settings, changes in deep percolation caused by  
377 pumping reductions do not significantly impact recharge rates within the 80-year projection  
378 period because recharge rates are low to begin with and changes in deep percolation take a long  
379 time to propagate down to the water table (Figure 8a). Following reductions in pumping, water  
380 table decline rates undergo an initial dramatic reduction then increase through time before  
381 stabilizing at an intermediate rate, consistent with our hypothesis (Figure 1). The increase occurs  
382 because the initial reduction within the conservation area creates a lateral hydraulic gradient that  
383 drives lateral flow into the surrounding non-conservation area; this phenomenon is further  
384 discussed in Section 3.3. In the lateral flow-dominated case, high fluxes of net lateral inflow  
385 compensate for the lack of recharge. This case only applies when  $K_z$  values are low as any

386 increase in recharge would add too much water to the aquifer, resulting in unrealistic rises in the  
387 water table. When LI is the controlling mechanism, the Brooks and Corey  $\epsilon$  has a negligible  
388 impact on the effectiveness of the pumping reductions.

389           In recharge-dominated cases, deep percolation can travel through the unsaturated zone  
390 rapidly enough that changes in applied irrigation water can alter the rate of groundwater recharge  
391 within our simulation period. Reductions in pumping decrease the amount of water that is  
392 applied in excess of crop water demands, and thus reduce the rate of deep percolation (Figure  
393 4b). Unlike the lateral flow-dominated case where there is no difference in recharge between the  
394 conservation and non-conservation areas over the time span of this analysis, the effects of  
395 changing deep percolation led to a reduction in groundwater recharge within the conservation  
396 area relative to the non-conservation area (Figure 8b). Once recharge decreases in response to the  
397 reduced pumping condition, water table decline rates increase, consistent with our hypothesis  
398 (Figure 1). However, even in recharge-dominated settings, conservation can lead to substantial  
399 changes in transect-parallel lateral outflows. These lateral outflows across the border of the  
400 conservation area reach up to  $\sim 25 \text{ mm yr}^{-1}$ , which is comparable to the difference in recharge  
401 between the conservation and non-conservation areas (Figure 8b).

402

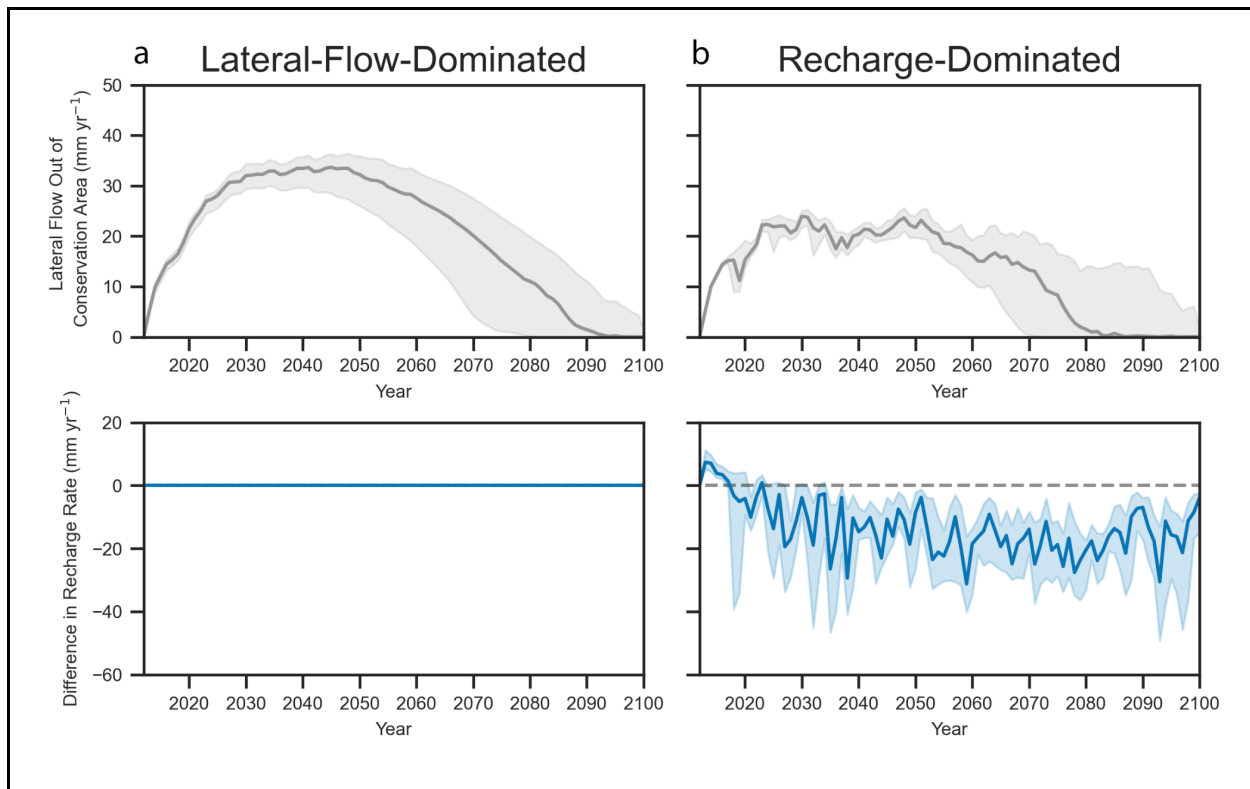


Figure 8: Average time series of simulated lateral outflow from the conservation area to the non-conservation area (gray lines, upper plots) and difference in recharge rate between the conservation area and the non-conservation area (blue lines, lower plots) for a) the lateral-flow-dominated and b) recharge-dominated cases. Thick lines represent average values across all model runs used for the projections and the shading indicates the interquartile range.

403  
 404 Lateral flow and recharge have distinct time lags from the onset of groundwater  
 405 conservation measures. For the lateral-flow-dominated cases, flow out of the conservation area  
 406 begins with the start of pumping reductions and increases quickly with the development of a  
 407 head gradient between the conservation and non-conservation areas. Eventually, lateral outflow  
 408 peaks at a rate of  $\sim 34 \text{ mm yr}^{-1}$  from 2030 to 2050, or  $\sim 17$  to  $\sim 37$  years after the onset of  
 409 conservation (Figure 8a). After 2050, lateral outflow gradually decreases due to a decline in the  
 410 head gradient between the conservation and non-conservation areas, typically reaching  $0 \text{ mm yr}^{-1}$   
 411 between 2080 and 2100 depending on the case. In the recharge-dominated cases (Figure 8b),  
 412 lateral flow out of the conservation area follows a similar pattern, though with a lower peak ( $\sim 24$

413 mm yr<sup>-1</sup>) and more interannual variability. The interannual variability in lateral outflows in the  
414 recharge-dominated cases is due to differences in recharge rates between the conservation and  
415 non-conservation areas, with larger lateral outflows when the recharge differences between the  
416 conservation and non-conservation areas are greater because this induces a larger hydraulic  
417 gradient between the two areas. For the recharge-dominated cases, there is an immediate short  
418 lived-period of positive differences in recharge rates, with recharge into the conservation area  
419 greater than into the non-conservation area because the reduction in water table decline rates  
420 allows more recharge to reach the water table than at higher decline rates. After five years,  
421 recharge rates in the groundwater conservation area adjust to the lower deep percolation rates  
422 associated with the reduced pumping condition, resulting in a negative difference for the rest of  
423 the simulation.

424         These differences between the lateral- and recharge-dominated cases indicate that, in  
425 settings with higher values of  $K_Z$  (in our case,  $> 0.0035 \text{ m d}^{-1}$ ; Figure 6), excess applied irrigation  
426 water can traverse the thick vadose zone that is present in western Kansas and ultimately  
427 recharge the water table. However, vertical hydraulic conductivity is not the only controlling  
428 factor in the recharge-dominated cases, as  $LI$ ,  $S_Y$ , and Brooks and Corey  $\epsilon$  also play important  
429 roles in the long-term effectiveness (see Figure 6). In cases where  $S_Y$  is low, high-performing  
430 parameter sets tend to have a greater  $LI$  to compensate for the low drainable pore space. When  
431  $K_Z$  values are low, Brooks and Corey  $\epsilon$  values must be low as well to allow for the calculated  
432 unsaturated hydraulic conductivity value to be high enough to transmit water through the vadose  
433 zone at a rapid enough rate to initiate groundwater recharge. As  $K_Z$  increases, so must the Brooks  
434 and Corey  $\epsilon$ , limiting the value of unsaturated hydraulic conductivity and preventing the aquifer  
435 from becoming inundated with excess water.

### 436 *3.3 Effects of lagged responses on aquifer usable lifetime*

437           These lagged responses to groundwater conservation led to different estimates of the  
438 degree to which conservation extends the usable aquifer lifetime. The lateral-flow-dominated  
439 cases had an average extension of 15 years for a 20% pumping reduction and an average  
440 extension of 25 years for a 30% reduction (Figure 9a, c). Results were similar for the recharge-  
441 dominated cases, where the average extension was 12 years with a reduction in pumping of 20%  
442 and 20 years for a pumping reduction of 30% (Figure 9b, d). Using the start of the initial SD-6  
443 LEMA in 2013, the remaining usable lifetime can be quantified. For the recharge-dominated  
444 cases, if no pumping reductions are applied, the water table will fall below eight meters of  
445 saturated thickness (the minimum thickness capable of supporting irrigated agriculture; Butler et  
446 al., 2020b) in 2047. If pumping is reduced by 20% or 30%, the aquifer lifetime will be extended  
447 to 2059 and 2067, respectively. For the lateral-flow-dominated cases, the water table will fall  
448 below eight meters of saturated thickness in 2045 in the absence of pumping reductions. With a  
449 20% and 30% pumping reduction, the lifetime is extended to 2060 and 2070, respectively. The  
450 numbers found in this study are within the envelope found by Butler et al. (2020b) who used a  
451 water balance approach to quantify the extension of usable lifetime under various exploratory  
452 scenarios, but does not differentiate between lagged changes in recharge and lateral flow. Our  
453 analysis extends this previous work by quantifying the relative importance of these two drivers  
454 of long-term change in net inflows.

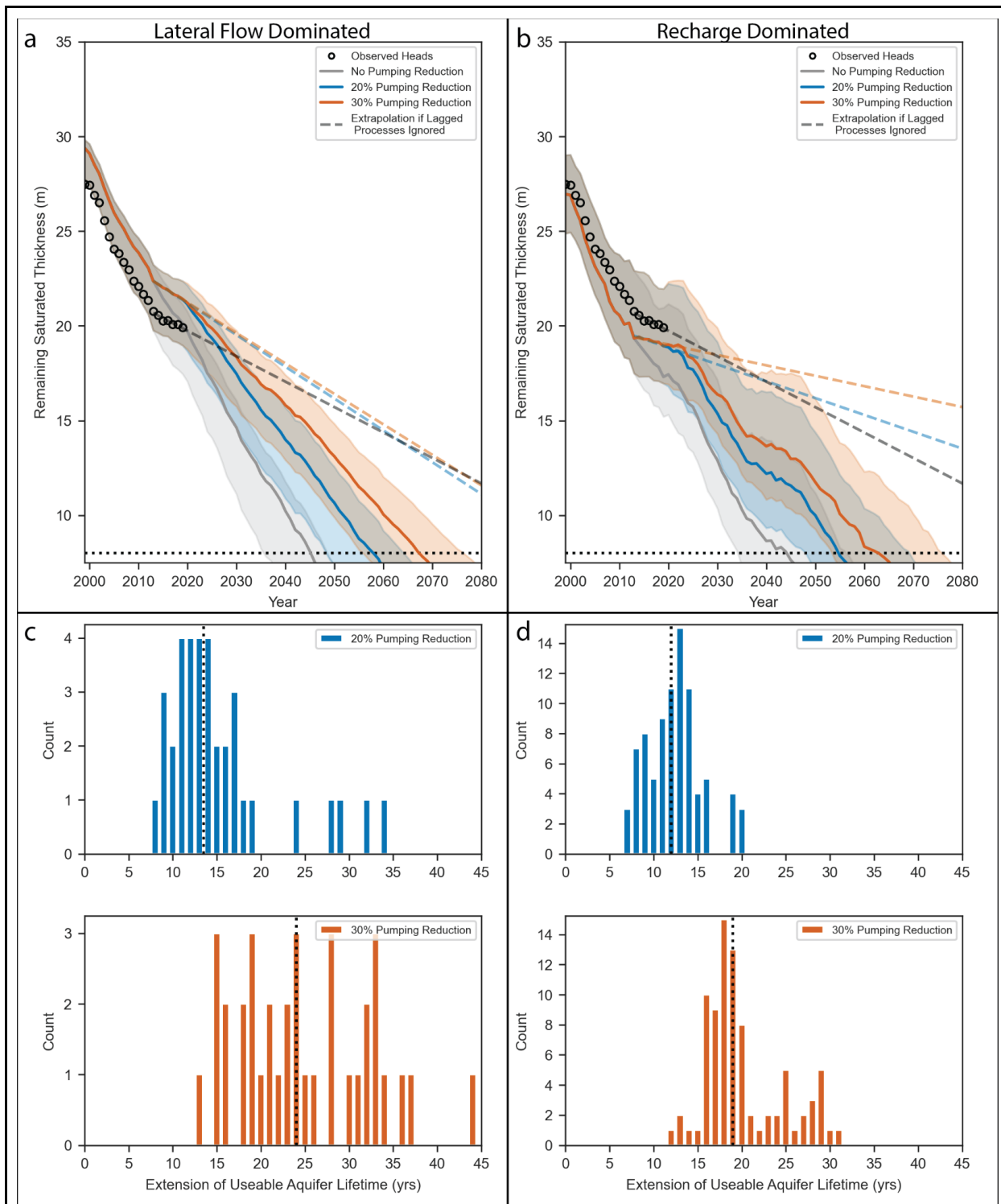


Figure 9: a) and b): Median simulated saturated thickness for the three pumping scenarios for a) lateral-flow-dominated and b) recharge-dominated cases. Dashed lines represent extrapolated remaining saturated thickness if the impact of lagged responses is ignored. The horizontal dotted line represents the minimum saturated thickness (eight meters) needed for large-scale

irrigated agriculture. c) and d): Median extension of usable lifetime (vertical black dotted line) and histogram of number of occurrences for the 20% and 30% pumping reduction scenarios for c) lateral-flow-dominated and d) recharge-dominated cases. Shaded areas in panels a) and b) represent the interquartile range of the simulated projections.

455

456

457

458

459

460

461

462

463

464

465

466

467

468

469

470

471

472

473

474

In general, these results indicate that the effectiveness of groundwater conservation could be overestimated if only using data from the period between initiation of pumping reductions and the onset of the lagged responses. Using the observed heads from 2013 to 2019 and extrapolating until the aquifer thickness drops below eight meters, the usable lifetime extends to 2107 (Figure 9a,b black dashed line). For the lateral flow-dominated cases, this value drops to 2098 for the 20% pumping reduction scenario and 2102 for the 30% pumping reduction scenario (Figure 9a, blue and orange dashed lines). The recharge-dominated cases result in a much greater duration with the usable lifetime extending to 2142 for the 20% pumping reduction case and 2220 for the 30% pumping reduction case (Figure 9b, blue and orange dashed lines). Ignoring the impacts of lagged responses by extrapolating the initial aquifer response to pumping reductions results in a dramatic overestimate of the effectiveness of these conservation methods. The subsequent increase in the water table decline rate dictates the long term effectiveness of groundwater conservation strategies. Understanding the mechanisms that control these lagged responses can manage stakeholder expectations and lead to the design of more effective conservation strategies that can further extend the usable lifetime of stressed aquifers. For example, as the effectiveness of initial conservation measures wanes and a return to increased water table decline rates begin to be observed, Butler et al. (2020b) have shown that additional pumping reductions can further extend usable aquifer lifetimes.

### 475 *3.4 Implications for isolated conservation areas within heavily stressed regional aquifers*

476 Conservation strategies are most urgently needed in heavily stressed aquifers. Since  
477 changes to groundwater flow can transmit the impacts of land use decisions to neighboring parts  
478 of the landscape (Zipper et al., 2017), it is important to understand how impacts of pumping  
479 reductions could extend beyond the borders of the conservation area. We found that changes in  
480 transect-parallel lateral flow caused by conservation can subsidize those outside the conservation  
481 area by slowing the rate of aquifer decline in the non-conservation area (Figure 10). As our  
482 modeling setup is symmetric, the largest extension of usable lifetime occurs in the center of the  
483 conservation area (values plotted in Figure 9) and decreases towards and across the boundary  
484 between the conservation and non-conservation areas. These cross-boundary effects are greatest  
485 under the transect-perpendicular lateral flow-dominated cases but also occur in recharge-  
486 dominated cases due to the transect-parallel lateral hydraulic gradient changes discussed above.  
487 Without any reductions in pumping outside the conservation area, the non-conservation area  
488 gains at least 5 years of additional usable aquifer lifetime at distances of approximately 2 km  
489 from the boundary for the 20% pumping reduction case and between 3.5 and 4 km for the 30%  
490 pumping reduction case. Extensions of the usable aquifer lifetime at 7 km from the boundary  
491 range between about 0.75 and 2 years. Effectively, the gains in usable aquifer lifetime brought  
492 about by conservation can spill out of the conservation area, indicating that the benefits of  
493 pumping reductions may extend beyond the borders of conservation areas by subsidizing their  
494 neighbors. However, the magnitude of this effect is likely dependent on the horizontal  
495 conductivity value and the size and shape of the conservation area. We would anticipate a  
496 smaller transect-parallel lateral flow subsidy in areas with a lower horizontal hydraulic

497 conductivity and/or a smaller perimeter-to-area ratio relative to the conditions simulated here,  
498 which would result in a longer extension of usable aquifer lifetime in the conservation area.

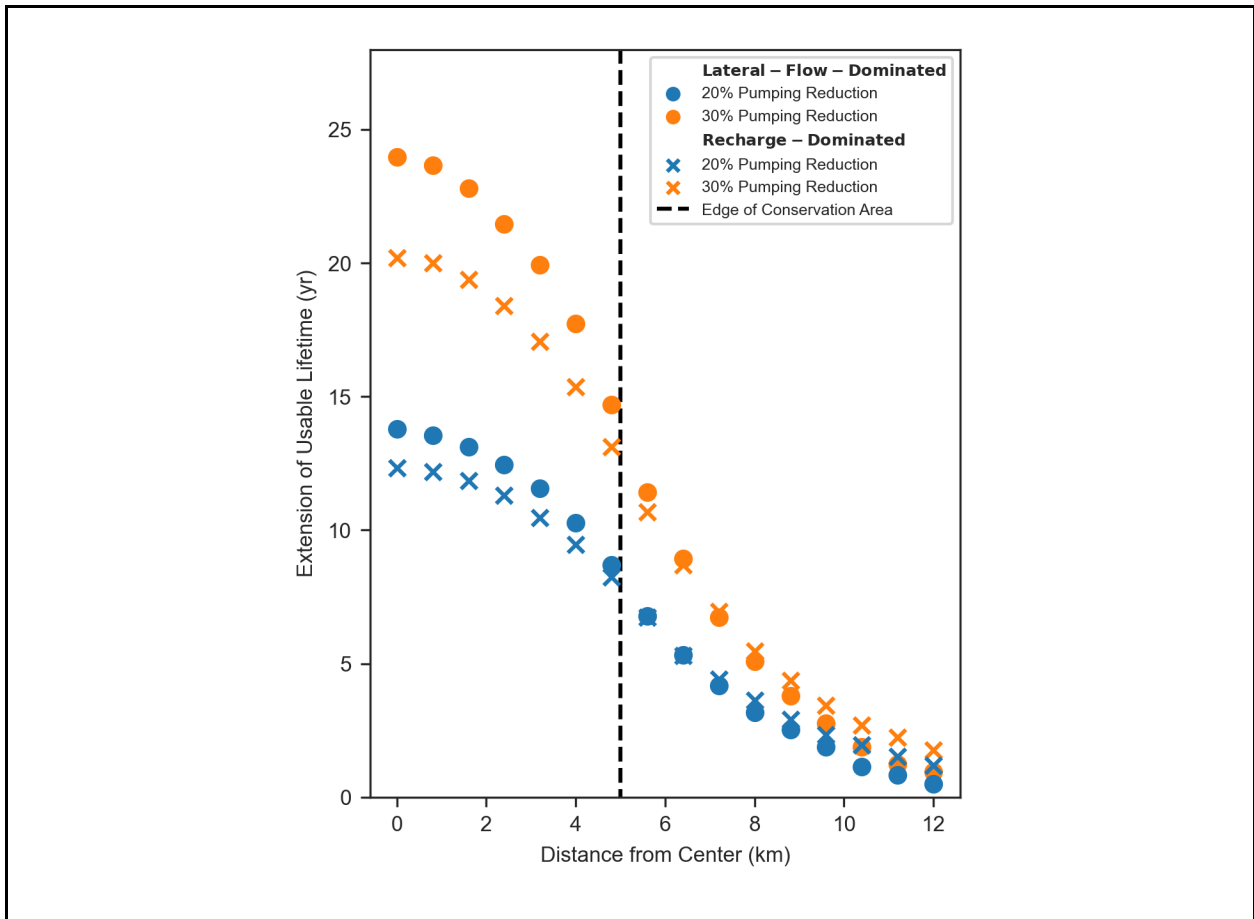


Figure 10: Average extension of usable aquifer lifetime for the lateral-flow-dominated (circles) and recharge-dominated (Xs) scenarios compared to distance from the center of the conservation area. Extension of usable aquifer lifetime was quantified for the center of each grid cell by calculating the difference in time between when the “No Conservation” scenario and the 20% and 30% pumping reduction scenarios reached eight meters of saturated thickness, which is the minimum saturated thickness capable of supporting large-scale pumping.

499  
500 While our surrogate model simulations found net outflow across the LEMA boundary, in  
501 practice many overexploited areas where groundwater conservation measures may be  
502 implemented are closed basins and therefore this may manifest through other impacts such as a  
503 reduction in cross-boundary inflows to the conservation area (Pauloo et al., 2021). In either case,

504 this indicates that the benefits of pumping reductions can extend beyond the boundaries of the  
505 areas with groundwater conservation initiatives, with potential socio-political impacts. Since  
506 heavily-pumped areas may preferentially exist in high productive aquifers with high  
507 transmissivity, the lateral cross-boundary effects we identify here are likely possible in many  
508 stressed aquifers. For instance, if pumping reductions are implemented in trans-boundary  
509 aquifers, lagged responses should be accounted for to ensure that water resources are shared  
510 equitably (Callegary et al., 2018; Lee et al., 2018; Lipponen & Chilton, 2018; Sindico et al.,  
511 2018).

### 512 ***3.5 Limitations and future research needs***

513 Although the modeling framework presented here reproduced the interannual and annual  
514 dynamics of the observed natural system (Figure 7), there are several limitations to our approach  
515 that may affect the results. First, aquifers are inherently complex, spatially heterogeneous, and  
516 frequently lack sufficient observation data. Our analysis deliberately simplified this complexity  
517 into a homogeneous surrogate model in order to isolate the role of lagged hydrological responses  
518 in areas of groundwater conservation, and therefore does not capture the intricacies of the natural  
519 world, such as spatial changes in depth to bedrock, strata discontinuity, incorporation of regional  
520 groundwater gradients, or heterogeneous distributions of pumping wells. However, our  
521 sensitivity analysis demonstrated that our conclusions were robust to these simplifications (see  
522 Text S1, Figure S5, and Table S1 for details). Because our surrogate model was based on the  
523 conditions and dimensions of an area with a specific groundwater conservation program, the  
524 exact thresholds identified in this study may not translate to other aquifer systems and should be  
525 viewed in the context of this study, which is to identify how lagged processes influence  
526 groundwater conservation initiatives. However, regardless of the specific thresholds, we would

527 expect the general relationships among variables to be consistent (e.g., lagged changes in  
528 recharge become more important in settings with greater vertical hydraulic conductivity).

529         Second, the applied pumping and deep percolation rates are based on statistical  
530 relationships using limited data. While Kansas has the most robust pumping well metering data  
531 in the United States (Foster et al., 2020; USDA National Agricultural Statistics Service, 2019),  
532 pumping rates for the period from 1955 to 1992 are based on a regression model while rates from  
533 1993 to 2019 are based on observed data. Additionally, when developing the projected pumping  
534 rates, we assumed that irrigation efficiency does not change and that neither the conservation nor  
535 the non-conservation areas change their pumping practices, which may not be the case as new  
536 technologies are adopted by or groundwater resources begin to become less accessible to the  
537 agricultural community. Applied deep percolation rates were developed using ten years of  
538 modeled data and extrapolated to fill the historical record, which may have resulted in deep  
539 percolation rates that are too high. We also assumed that the (transect-perpendicular) east-to-  
540 west lateral inflows to the system are constant through time. These issues point to a critical need  
541 to better monitor vertical fluxes of water in deep vadose zones and lateral fluxes in aquifers to  
542 inform future modeling efforts and conservation program evaluations.

543         Third, the use of the UZF package to simulate variably saturated flow is limited in several  
544 aspects. If applied deep percolation rates are greater than the prescribed saturated hydraulic  
545 conductivity, excess water is removed from the system, as low hydraulic conductivity conditions  
546 typical of lateral-flow-dominated cases are limited not just by the rate at which water percolates  
547 through the unsaturated zone, but also by the supply of water able to infiltrate into the root zone.  
548 Incorporating heterogeneity into the model domain was not possible with the UZF package as it  
549 can only be applied to one active layer, further simplifying the representation. We had attempted

550 to address this limitation by using another MODFLOW-based variably-saturated flow solution,  
551 HYDRUS Package for MODFLOW (Beegum et al., 2018; Seo et al., 2007), which solves a 1-D  
552 unsaturated Richards Equation for each cell column, but experienced both instability and  
553 anomalous results that prevented its application here. Finally, all projection results are based on  
554 randomly sampling the historical record of precipitation to generate time series for deep  
555 percolation and pumping, which provides realistic daily meteorological dynamics but inherently  
556 ignores climate change impacts and implications.

557         Although our modeling approach may disregard some locally important heterogeneity,  
558 our objective was to analyze the major factors controlling the long-term effectiveness of  
559 groundwater conservation initiatives. Our simplified surrogate modeling approach allows for the  
560 fundamental processes to be investigated while removing the impact of site specific phenomena,  
561 ultimately allowing for a more generalized understanding of aquifer system dynamics that can be  
562 transferred to other aquifers that are at risk of depletion. Applying these assumptions, we were  
563 able to investigate the interplay among vertical hydraulic conductivity, soil water retention  
564 properties, lateral flows, and recharge. This allowed us to assess the long-term effectiveness of  
565 pumping reduction based groundwater conservation strategies, and estimate the extension of the  
566 usable aquifer lifetime for both the lateral-flow- and recharge-dominated cases.

#### 567 **4. Conclusions**

568         Pumping reductions are, in many settings, the only viable method for extending the  
569 lifetime of groundwater resources. In this study, we demonstrate that pumping reductions can  
570 lead to changes in lateral groundwater flow and recharge, and these lagged responses to pumping  
571 reductions ultimately have a substantial influence over the long-term effectiveness of  
572 groundwater conservation initiatives. The degree to which lateral flow and recharge impact long-

573 term effectiveness is strongly dependent on the vertical hydraulic conductivity of the unsaturated  
574 zone, which controls the degree to which changes in deep percolation can translate into changes  
575 in groundwater recharge. We found that larger reductions in pumping result in a longer extension  
576 of the usable aquifer lifetime, and that this impact is most strongly felt in the center of the  
577 conservation area and that the benefits of groundwater conservation programs may extend  
578 beyond the areas implementing conservation practices due to lateral flow. However, we  
579 anticipate that the impact of lateral flow will lessen as the size of the conservation area increases  
580 and its perimeter-to-area ratio decreases. Thus, this work should be considered an initial step in  
581 assessing the interplay between the various mechanisms controlling an aquifer's response to  
582 pumping-based conservation initiatives.

### 583 **Acknowledgments**

584 This work was supported, in part, by the United States Department of Agriculture  
585 (USDA) under USDA-NIFA grant 2018-67003-27406 and subaward RC104693B, the USDA  
586 and the National Science Foundation (NSF) under USDA-NIFA/NSF-INFIEWS grant 2018-  
587 67003-27406subaward RC108063UK, and the NSF under Grant No. 2108196. Any opinions,  
588 findings, and conclusions or recommendations expressed in this material are those of the authors  
589 and do not necessarily reflect the views of the USDA or NSF. We would like to thank Geoff  
590 Bohling and Brownie Wilson for their help procuring data and helpful comments. Data and code  
591 are available at [https://github.com/tomglose/SD6\\_Modeling\\_Project.git](https://github.com/tomglose/SD6_Modeling_Project.git) during the review  
592 process and will be placed in a repository at the time of paper acceptance.

593

594

595

596 **References**

- 597 Abatzoglou, J. T. (2013). Development of gridded surface meteorological data for ecological  
598 applications and modelling. *International Journal of Climatology*, 33(1), 121–131.  
599 <https://doi.org/10.1002/joc.3413>
- 600 Asher, M. J., Croke, B. F. W., Jakeman, A. J., & Peeters, L. J. M. (2015). A review of surrogate  
601 models and their application to groundwater modeling. *Water Resources Research*, 51(8),  
602 5957–5973. <https://doi.org/10.1002/2015WR016967>
- 603 Bailey, R. T., Morway, E. D., Niswonger, R. G., & Gates, T. K. (2013). Modeling Variably  
604 Saturated Multispecies Reactive Groundwater Solute Transport with MODFLOW-UZF  
605 and RT3D. *Groundwater*, 51(5), 752–761. [https://doi.org/10.1111/j.1745-](https://doi.org/10.1111/j.1745-6584.2012.01009.x)  
606 [6584.2012.01009.x](https://doi.org/10.1111/j.1745-6584.2012.01009.x)
- 607 Bakker, M., Post, V., Langevin, C. D., Hughes, J. D., White, J. T., Starn, J. J., & Fienen, M. N.  
608 (2016). Scripting MODFLOW Model Development Using Python and FloPy.  
609 *Groundwater*, 54(5), 733–739. <https://doi.org/10.1111/gwat.12413>
- 610 Beegum, S., Šimůnek, J., Szymkiewicz, A., Sudheer, K. P., & Nambi, I. M. (2018). Updating the  
611 Coupling Algorithm between HYDRUS and MODFLOW in the HYDRUS Package for  
612 MODFLOW. *Vadose Zone Journal*, 17(1), 180034.  
613 <https://doi.org/10.2136/vzj2018.02.0034>
- 614 Beven, K. (2006). A manifesto for the equifinality thesis. *The Model Parameter Estimation*  
615 *Experiment*, 320(1), 18–36. <https://doi.org/10.1016/j.jhydrol.2005.07.007>
- 616 Bierkens, M. F. P., & Wada, Y. (2019). Non-renewable groundwater use and groundwater  
617 depletion: a review. *Environmental Research Letters*, 14(6), 063002.  
618 <https://doi.org/10.1088/1748-9326/ab1a5f>

619 Brooks, R. H., & Corey, A. T. (1966). Properties of porous media affecting fluid flow. *Journal of*  
620 *the Irrigation and Drainage Division*, 92(2), 61–90.

621 Butler, J. J., Jr., Whittemore, D. O., Wilson, B. B., & Bohling, G. C. (2016). A new approach for  
622 assessing the future of aquifers supporting irrigated agriculture. *Geophysical Research*  
623 *Letters*, 43(5), 2004–2010. <https://doi.org/10.1002/2016GL067879>

624 Butler, J. J., Jr., Whittemore, D. O., Reboulet, E. C., Knobbe, S., Wilson, B. B., & Bohling, G. C.  
625 (2019). High Plains aquifer index well program: 2019 annual report.

626 Butler, J. J., Jr., Bohling, G. C., Whittemore, D. O., & Wilson, B. B. (2020a). A roadblock on the  
627 path to aquifer sustainability: underestimating the impact of pumping reductions.  
628 *Environmental Research Letters*, 15(1), 014003. [https://doi.org/10.1088/1748-](https://doi.org/10.1088/1748-9326/ab6002)  
629 [9326/ab6002](https://doi.org/10.1088/1748-9326/ab6002)

630 Butler, J. J., Jr., Bohling, G. C., Whittemore, D. O., & Wilson, B. B. (2020b). Charting Pathways  
631 Toward Sustainability for Aquifers Supporting Irrigated Agriculture. *Water Resources*  
632 *Research*, 56(10), e2020WR027961. <https://doi.org/10.1029/2020WR027961>

633 Callegary, J. B., Megdal, S. B., Tapia Villaseñor, E. M., Petersen-Perlman, J. D., Minjárez Sosa,  
634 I., Monreal, R., et al. (2018). Findings and lessons learned from the assessment of the  
635 Mexico-United States transboundary San Pedro and Santa Cruz aquifers: The utility of  
636 social science in applied hydrologic research. *Special Issue on International Shared*  
637 *Aquifer Resources Assessment and Management*, 20, 60–73.  
638 <https://doi.org/10.1016/j.ejrh.2018.08.002>

639 Castilla-Rho, J. C., Rojas, R., Andersen, M. S., Holley, C., & Mariethoz, G. (2019). Sustainable  
640 groundwater management: How long and what will it take? *Global Environmental*  
641 *Change*, 58, 101972. <https://doi.org/10.1016/j.gloenvcha.2019.101972>

642 Deines, J. M., Kendall, A. D., Butler, J. J., Jr., & Hyndman, D. W. (2019). Quantifying irrigation  
643 adaptation strategies in response to stakeholder-driven groundwater management in the  
644 US High Plains Aquifer. *Environmental Research Letters*, *14*, 044014.  
645 <https://doi.org/10.1088/1748-9326/aafe39>

646 Deines, J. M., Schipanski, M. E., Golden, B., Zipper, S. C., Nozari, S., Rottler, C., et al. (2020).  
647 Transitions from irrigated to dryland agriculture in the Ogallala Aquifer: Land use  
648 suitability and regional economic impacts. *Agricultural Water Management*, *233*,  
649 106061. <https://doi.org/10.1016/j.agwat.2020.106061>

650 Deines, J. M., Kendall, A. D., Butler, J. J., Jr., Basso, B., & Hyndman, D. W. (2021). Combining  
651 Remote Sensing and Crop Models to Assess the Sustainability of Stakeholder-Driven  
652 Groundwater Management in the US High Plains Aquifer. *Water Resources Research*,  
653 e2020WR027756. <https://doi.org/10.1029/2020WR027756>

654 DeSimone, L. A., McMahon, P. B., & Rosen, M. R. (2015). *The quality of our Nation's waters:*  
655 *Water quality in principal aquifers of the United States, 1991-2010* (Report No. 1360) (p.  
656 161). Reston, VA. <https://doi.org/10.3133/cir1360>

657 Dieter, C. A., Maupin, M. A., Caldwell, R. R., Harris, M. A., Ivahnenko, T. I., Lovelace, J. K., et  
658 al. (2018). *Estimated use of water in the United States in 2015* (Report No. 1441) (p. 76).  
659 Reston, VA. <https://doi.org/10.3133/cir1441>

660 Doherty, J. (2015). *Calibration and uncertainty analysis for complex environmental models*.  
661 Watermark Numerical Computing Brisbane, Australia.

662 Foster, T., Brozović, N., & Butler, A. P. (2017). Effects of initial aquifer conditions on economic  
663 benefits from groundwater conservation. *Water Resources Research*, *53*(1), 744–762.  
664 <https://doi.org/10.1002/2016WR019365>

665 Foster, T., Mieno, T., & Brozović, N. (2020). Satellite-Based Monitoring of Irrigation Water  
666 Use: Assessing Measurement Errors and Their Implications for Agricultural Water  
667 Management Policy. *Water Resources Research*, 56(11), e2020WR028378.  
668 <https://doi.org/10.1029/2020WR028378>

669 Fross, D., Sophocleous, M. A., Wilson, B. B., & Butler, J. J., Jr. (2012). Kansas High Plains  
670 Aquifer Atlas, Kansas Geological Survey. Retrieved from  
671 [http://www.kgs.ku.edu/HighPlains/HPA\\_Atlas/index.html](http://www.kgs.ku.edu/HighPlains/HPA_Atlas/index.html)

672 Gleeson, T., Alley, W. M., Allen, D. M., Sophocleous, M. A., Zhou, Y., Taniguchi, M., &  
673 VanderSteen, J. (2012). Towards sustainable groundwater use: setting long-term goals,  
674 backcasting, and managing adaptively. *Ground Water*, 50(1), 19–26.  
675 <https://doi.org/10.1111/j.1745-6584.2011.00825.x>

676 Gleeson, T., Cuthbert, M., Ferguson, G., & Perrone, D. (2020). Global Groundwater  
677 Sustainability, Resources, and Systems in the Anthropocene. *Annual Review of Earth and*  
678 *Planetary Sciences*, 48(1), 431–463. [https://doi.org/10.1146/annurev-earth-071719-](https://doi.org/10.1146/annurev-earth-071719-055251)  
679 [055251](https://doi.org/10.1146/annurev-earth-071719-055251)

680 Golden, B. (2018). *Monitoring the Impacts of Sheridan County 6 Local Enhanced Management*  
681 *Area: Final Report for 2013 – 2017*. Manhattan, KS. Retrieved from  
682 [https://agriculture.ks.gov/docs/default-source/dwr-water-appropriation-](https://agriculture.ks.gov/docs/default-source/dwr-water-appropriation-documents/sheridancounty6_lemma_goldenreport_2013-2017.pdf?sfvrsn=dac48ac1_0)  
683 [documents/sheridancounty6\\_lemma\\_goldenreport\\_2013-2017.pdf?sfvrsn=dac48ac1\\_0](https://agriculture.ks.gov/docs/default-source/dwr-water-appropriation-documents/sheridancounty6_lemma_goldenreport_2013-2017.pdf?sfvrsn=dac48ac1_0)

684 Gurdak, J. J., Walvoord, M. A., & McMahon, P. B. (2008). Susceptibility to Enhanced Chemical  
685 Migration from Depression-Focused Preferential Flow, High Plains Aquifer. *Vadose*  
686 *Zone Journal*, 7(4), 1218–1230. <https://doi.org/10.2136/vzj2007.0145>

687 Hansen, C. V. (1991). *Estimates of freshwater storage and potential natural recharge for*

688            *principal aquifers in Kansas* (Report No. 87-4230). <https://doi.org/10.3133/wri874230>

689    Hou, X., Wang, S., Jin, X., Li, M., Lv, M., & Feng, W. (2020). Using an ETWatch (RS)-UZFL  
690            MODFLOW Coupled Model to Optimize Joint Use of Transferred Water and Local  
691            Water Sources in a Saline Water Area of the North China Plain. *Water*, 12(12), 3361.

692    Hu, Y., Moiwo, J. P., Yang, Y., Han, S., & Yang, Y. (2010). Agricultural water-saving and  
693            sustainable groundwater management in Shijiazhuang Irrigation District, North China  
694            Plain. *Journal of Hydrology*, 393(3), 219-232.  
695            <https://doi.org/10.1016/j.jhydrol.2010.08.017>

696    Huggins, X., Gleeson, T., Kummu, M., Zipper, S. C., Wada, Y., Troy, T. J., & Famiglietti, J. S.  
697            (2022). Hotspots for social and ecological impacts from freshwater stress and storage  
698            loss. *Nature Communications*, 13(1), 439. <https://doi.org/10.1038/s41467-022-28029-w>

699    Hunt, R. J., Prudic, D. E., Walker, J. F., & Anderson, M. P. (2008). Importance of Unsaturated  
700            Zone Flow for Simulating Recharge in a Humid Climate. *Groundwater*, 46(4), 551-560.  
701            <https://doi.org/10.1111/j.1745-6584.2007.00427.x>

702    Kansas Department of Agriculture. (2013). Order of designation approving the Sheridan 6 Local  
703            Enhanced Management Area within Groundwater Management District No. 4. Retrieved  
704            from [https://sftp.kda.ks.gov:4443/LEMAs/SD6/LEMA.SD6.OrderOfDesignation.2013](https://sftp.kda.ks.gov:4443/LEMAs/SD6/LEMA.SD6.OrderOfDesignation.20130417.pdf)  
705            0417.pdf

706    Kansas Department of Agriculture. (2018). Order of designation regarding the Groundwater  
707            Management District No. 4 District Wide Local Enhanced Management Plan. Retrieved  
708            from [https://agriculture.ks.gov/docs/default-source/dwr-water-appropriation-](https://agriculture.ks.gov/docs/default-source/dwr-water-appropriation-documents/gmd4_lemma_orderofdesignation.pdf?sfvrsn=30e981c1_4)  
709            documents/gmd4\_lemma\_orderofdesignation.pdf?sfvrsn=30e981c1\_4

710    Kansas Department of Agriculture. (2021). Order of designation regarding the Management Plan

711 for the Wichita County Local Enhanced Management Area. Retrieved from  
712 <https://agriculture.ks.gov/docs/default-source/dwr-water-appropriation-documents/whc->  
713 [lema-order-of-designation---final.pdf?sfvrsn=60d690c1\\_0](https://agriculture.ks.gov/docs/default-source/dwr-water-appropriation-documents/whc-)  
714 Kansas Statutes Annotated 82a-1041. (2012). Local enhanced management areas; establishment  
715 procedures; duties of chief engineer; hearing; notice; orders; review. Retrieved from  
716 [http://www.ksrevisor.org/statutes/chapters/ch82a/082a\\_010\\_0041.html](http://www.ksrevisor.org/statutes/chapters/ch82a/082a_010_0041.html)  
717 Katz, B. S., Stotler, R. L., Hirmas, D., Ludvigson, G., Smith, J. J., & Whittemore, D. O. (2016).  
718 Geochemical Recharge Estimation and the Effects of a Declining Water Table. *Vadose*  
719 *Zone Journal*, 15(vzj2016.04.0031). <https://doi.org/10.2136/vzj2016.04.0031>  
720 Kennedy, J., Ferré, T. P. A., & Creutzfeldt, B. (2016). Time-lapse gravity data for monitoring  
721 and modeling artificial recharge through a thick unsaturated zone. *Water Resources*  
722 *Research*, 52(9), 7244–7261. <https://doi.org/10.1002/2016WR018770>  
723 Kling, H., Fuchs, M., & Paulin, M. (2012). Runoff conditions in the upper Danube basin under  
724 an ensemble of climate change scenarios. *Journal of Hydrology*, 424–425, 264–277.  
725 <https://doi.org/10.1016/j.jhydrol.2012.01.011>  
726 Konikow, L. F., & Bredehoeft, J. D. (1992). Ground-water models cannot be validated.  
727 *Validation of Geo-Hydrological Models Part 1*, 15(1), 75–83.  
728 [https://doi.org/10.1016/0309-1708\(92\)90033-X](https://doi.org/10.1016/0309-1708(92)90033-X)  
729 Lee, E., Jayakumar, R., Shrestha, S., & Han, Z. (2018). Assessment of transboundary aquifer  
730 resources in Asia: Status and progress towards sustainable groundwater management.  
731 *Special Issue on International Shared Aquifer Resources Assessment and Management*,  
732 20, 103–115. <https://doi.org/10.1016/j.ejrh.2018.01.004>  
733 Lin, X., Harrington, J., Ciampitti, I., Gowda, P., Brown, D., & Kisekka, I. (2017). Kansas Trends

734 and Changes in Temperature, Precipitation, Drought, and Frost-Free Days from the 1890s  
735 to 2015. *Journal of Contemporary Water Research & Education*, 162(1), 18–30.  
736 <https://doi.org/10.1111/j.1936-704X.2017.03257.x>

737 Lipponen, A., & Chilton, J. (2018). Development of cooperation on managing transboundary  
738 groundwaters in the pan-European region: The role of international frameworks and joint  
739 assessments. *Special Issue on International Shared Aquifer Resources Assessment and*  
740 *Management*, 20, 145–157. <https://doi.org/10.1016/j.ejrh.2018.05.001>

741 Liu, G., Wilson, B. B., Bohling, G. C., Whittemore, D. O., & Butler Jr, J. J. (2022). Estimation  
742 of Specific Yield for Regional Groundwater Models: Pitfalls, Ramifications, and a  
743 Promising Path Forward. *Water Resources Research*, 58(1), e2021WR030761.  
744 <https://doi.org/10.1029/2021WR030761>

745 McKay, M. D., Beckman, R. J., & Conover, W. J. (1979). Comparison of Three Methods for  
746 Selecting Values of Input Variables in the Analysis of Output from a Computer Code.  
747 *Technometrics*, 21(2), 239–245. <https://doi.org/10.1080/00401706.1979.10489755>

748 McMahan, P. B., Dennehy, K. F., Bruce, B. W., Böhlke, J. K., Michel, R. L., Gurdak, J. J., &  
749 Hurlbut, D. B. (2006). Storage and transit time of chemicals in thick unsaturated zones  
750 under rangeland and irrigated cropland, High Plains, United States. *Water Resources*  
751 *Research*, 42(3). <https://doi.org/10.1029/2005WR004417>

752 Miro, M. E., & Famiglietti, J. S. (2019). A framework for quantifying sustainable yield under  
753 California’s Sustainable Groundwater Management Act (SGMA). *Sustainable Water*  
754 *Resources Management*, 5(3), 1165–1177.

755 Morway, E. D., Niswonger, R. G., Langevin, C. D., Bailey, R. T., & Healy, R. W. (2013).  
756 Modeling Variably Saturated Subsurface Solute Transport with MODFLOW-UZF and

757 MT3DMS. *Groundwater*, 51(2), 237–251. <https://doi.org/10.1111/j.1745->  
758 6584.2012.00971.x

759 Nazarieh, F., Ansari, H., Ziaei, A. N., Izady, A., Davari, K., & Brunner, P. (2018). Spatial and  
760 temporal dynamics of deep percolation, lag time and recharge in an irrigated semi-arid  
761 region. *Hydrogeology Journal*, 26(7), 2507–2520. <https://doi.org/10.1007/s10040-018->  
762 1789-z

763 Niswonger, R. G., & Prudic, D. E. (2009). Comment on “Evaluating Interactions between  
764 Groundwater and Vadose Zone Using the HYDRUS-Based Flow Package for  
765 MODFLOW” by Navin Kumar C. Twarakavi, Jirka Šimůnek, and Sophia Seo. *Vadose*  
766 *Zone Journal*, 8(3), 818–819. <https://doi.org/10.2136/vzj2008.0155>

767 Niswonger, R. G., Prudic, D. E., & Regan, R. S. (2006). *Documentation of the Unsaturated-Zone*  
768 *Flow (UZFI) Package for modeling Unsaturated Flow Between the Land Surface and the*  
769 *Water Table with MODFLOW-2005* (Report No. 6-A19). <https://doi.org/10.3133/tm6A19>

770 Pauloo, R. A., Fogg, G. E., Guo, Z., & Harter, T. (2021). Anthropogenic basin closure and  
771 groundwater salinization (ABCSAL). *Journal of Hydrology*, 593, 125787.  
772 <https://doi.org/10.1016/j.jhydrol.2020.125787>

773 Pfeiffer, L., & Lin, C.-Y. C. (2010). The effect of irrigation technology on groundwater use.  
774 *Choices*, 25(3), 1–6.

775 Poeter, E. P., & Hill, M. C. (1999). UCODE, a computer code for universal inverse modeling.  
776 *Computers & Geosciences*, 25(4), 457–462.

777 Razavi, S., Tolson, B. A., & Burn, D. H. (2012). Review of surrogate modeling in water  
778 resources. *Water Resources Research*, 48(7). <https://doi.org/10.1029/2011WR011527>

779 Rogers, D. H., & Lamm, F. R. (2012). Kansas irrigation trends. Presented at the Proceedings of

780 the 24th Annual Central Plains Irrigation Conference, Colby, Kansas, February 21-22,  
781 2012, Central Plains Irrigation Association.

782 Savenije, H. H. G. (2001). Equifinality, a blessing in disguise? *Hydrological Processes*, 15(14),  
783 2835–2838. <https://doi.org/10.1002/hyp.494>

784 Scanlon, B. R., Keese, K. E., Flint, A. L., Flint, L. E., Gaye, C. B., Edmunds, W. M., &  
785 Simmers, I. (2006). Global synthesis of groundwater recharge in semiarid and arid  
786 regions. *Hydrological Processes*, 20(15), 3335–3370. <https://doi.org/10.1002/hyp.6335>

787 Scanlon, B. R., Faunt, C. C., Longuevergne, L., Reedy, R. C., Alley, W. M., McGuire, V. L., &  
788 McMahon, P. B. (2012). Groundwater depletion and sustainability of irrigation in the US  
789 High Plains and Central Valley. *Proceedings of the National Academy of Sciences*,  
790 109(24), 9320–9325. <https://doi.org/10.1073/pnas.1200311109>

791 Seo, H. S., Simunek, J., & Poeter, E. P. (2007). Documentation of the hydrus package for  
792 modflow-2000, the us geological survey modular ground-water model. *IGWMC-*  
793 *International Ground Water Modeling Center*.

794 Sindico, F., Hirata, R., & Manganelli, A. (2018). The Guarani Aquifer System: From a Beacon  
795 of hope to a question mark in the governance of transboundary aquifers. *Special Issue on*  
796 *International Shared Aquifer Resources Assessment and Management*, 20, 49–59.  
797 <https://doi.org/10.1016/j.ejrh.2018.04.008>

798 Smith, R. (1983). Approximate soil water movement by kinematic characteristics. *Soil Science*  
799 *Society of America Journal*, 47(1), 3–8.

800 Smith, R., & Hebbert, R. H. B. (1983). Mathematical simulation of interdependent surface and  
801 subsurface hydrologic processes. *Water Resources Research*, 19(4), 987–1001.  
802 <https://doi.org/10.1029/WR019i004p00987>

803 USDA National Agricultural Statistics Service. (2019). 2018 Irrigation and water management  
804 survey, 3. Retrieved from  
805 [https://www.nass.usda.gov/Publications/AgCensus/2017/Online\\_Resources/Farm\\_and\\_R](https://www.nass.usda.gov/Publications/AgCensus/2017/Online_Resources/Farm_and_Ranch_Irrigation_Survey/fris.pdf)  
806 [anch\\_Irrigation\\_Survey/fris.pdf](https://www.nass.usda.gov/Publications/AgCensus/2017/Online_Resources/Farm_and_Ranch_Irrigation_Survey/fris.pdf)

807 Voss, C. I. (2011a). Editor's message: Groundwater modeling fantasies —part 1, adrift in the  
808 details. *Hydrogeology Journal*, 19(7), 1281–1284. [https://doi.org/10.1007/s10040-011-](https://doi.org/10.1007/s10040-011-0789-z)  
809 [0789-z](https://doi.org/10.1007/s10040-011-0789-z)

810 Voss, C. I. (2011b). Editor's message: Groundwater modeling fantasies—part 2, down to earth.  
811 *Hydrogeology Journal*, 19(8), 1455–1458. <https://doi.org/10.1007/s10040-011-0790-6>

812 Whittemore, D. O., Butler, J. J., Jr., & Wilson, B. B. (2018). Status of the High Plains Aquifer in  
813 Kansas. *Kansas Geological Survey Technical Series*, 22. Retrieved from  
814 [www.kgs.ku.edu/Publications/Bulletins/TS22/index.html](http://www.kgs.ku.edu/Publications/Bulletins/TS22/index.html)

815 Zell, W. O., & Sanford, W. E. (2020). Calibrated Simulation of the Long-Term Average Surficial  
816 Groundwater System and Derived Spatial Distributions of its Characteristics for the  
817 Contiguous United States. *Water Resources Research*, 56(8), e2019WR026724.  
818 <https://doi.org/10.1029/2019WR026724>

819 Zipper, S. C., Soylu, M. E., Kucharik, C. J., & II, S. P. L. (2017). Quantifying indirect  
820 groundwater-mediated effects of urbanization on agroecosystem productivity using  
821 MODFLOW-AgroIBIS (MAGI), a complete critical zone model. *Ecological Modelling*,  
822 359, 201–219. <https://doi.org/10.1016/j.ecolmodel.2017.06.002>

823 Zipper, S. C., Lamontagne-Hallé, P., McKenzie, J. M., & Rocha, A. V. (2018). Groundwater  
824 Controls on Postfire Permafrost Thaw: Water and Energy Balance Effects. *Journal of*  
825 *Geophysical Research: Earth Surface*, 123(10), 2677–2694.

826 <https://doi.org/10.1029/2018JF004611>

827 Zipper, S. C., Gleeson, T., Kerr, B., Howard, J. K., Rohde, M. M., Carah, J., & Zimmerman, J.

828 (2019). Rapid and Accurate Estimates of Streamflow Depletion Caused by Groundwater

829 Pumping Using Analytical Depletion Functions. *Water Resources Research*, 55(7), 5807–

830 5829. <https://doi.org/10.1029/2018WR024403>